Bruno Alfredo da Silva Branco

Licenciado em Ciências da Engenharia Electrotécnica e de Computadores

Multipacket Reception in LTE femtocell networks

Dissertação apresentada para obtenção do Grau de Mestre em Engenharia Electrotécnica e de Computadores, pela Universidade Nova de Lisboa, Faculdade de Ciências e Tecnologia.

Orientador : Luís Bernardo, Professor Auxiliar com Agregação , FCT-UNL
Rui Dinis, Professor Auxiliar com Agregação, FCT-UNL

Júri:
Presidente: Prof. Doutor Rodolfo Oliveira
Arguente: Prof. Doutor Rui Marinheiro
Vogais: Prof. Doutor Luís Bernardo
Prof. Doutor Rui Dinis

FACULDADE DE CIÊNCIAS E TECNOLOGIA
UNIVERSIDADE NOVA DE LISBOA

Setembro, 2013

Multipacket Reception in LTE femtocell networks

"Engineers like to solve problems. If there are no problems handily available, they will create their own problems." Scott Adams

Acknowledgements

I would like to thank my supervisors Prof. Luís Bernardo and Prof. Rui Dinis, for offering me the opportunity to work in this topic, for his patience and insightful guidance using equipment and other financing provided by FCT/MEC Femtocells(PTDC/EEA-TEL/120666/2010), OPPORTUNISTIC CR(PTDC/EEA-TEL/115981/2009) and ADIN (PTDC/EEI-TEL/2990/2012) projects. My special thanks to all my friends, and office mates for their support at the telecommunication laboratory for their fellowship, great ambiance and their advices to overcome all the difficulties during the thesis realization. Last but not least, my deepest gratitude to my parents and girlfriend, for their love, trust and support.

Sumário

A crescente procura por serviços sem fios de banda larga levou ao desenvolvimento e evolução das tecnologias de rede celular, que prometem ritmos elevados para utilizadores móveis. A 3GPP propôs o LTE (Long Term Evolution) e mais recentemente o LTE-A (LTE advanced). Está prevista a existência de macro estações base (eNB) e de micro estações (HeNB), com baixa potência que complementa a cobertura da rede aumentando a densidade de estações base. Com o inerente aumento da interferência, torna-se essencial uma receção eficaz. Nesta dissertação é proposta a utilização de SC-FDE no downlink de uma rede de femtocells e especialmente a utilização da receção multipacote (MPR) para fornecer serviços de alto débito sem fios. Por outro lado com as crescentes preocupações ambientais, surgiu o conceito de Green Communications (GC) que visa encontrar soluções para o melhoramento da eficiência energética das redes. Tendo como base os princípios de GC é proposto um algoritmo para controlar o número de estações base (principais responsáveis pelo consumo energético das rede sem fios) necessárias fornecer serviços com igual elevada qualidade. Os resultados globais mostram que as tecnologias empregues são uma solução para obter uma boa relação desempenho/poupança energética, indo ao encontro das exigências (elevadas taxas de dados) e das preocupações (baixo consumos de energia) da sociedade moderna.

Palavras Chave: *Long Term Evolution* (LTE), *Single Carrier with Frequency Domain Equalization* (SC-FDE), *Frequency-Domain Equalization* (FDE), *Iterative Block-Decision Feedback Equalizer* (IB-DFE), femtocell (*Home enhanced Node B* (HeNB)), *Successive Interference Cancellation* (SIC), *Multipacket Reception* (MPR), *Green Communications* (GC)

Abstract

Driven by the growing demand for high-speed broadband wireless services, LTE technology has emerged and evolve, promising high data rates to the demanding mobile users. Based on the *3rd Generation Partnership Project* (3GPP) specifications,*Long Term Evolution Advanced* (LTE-A) telecommunication services predict the existence of macro base stations, *Enhanced Node B* (eNB) and micro stations HeNB with low power that complements the network's coverage. This dissertation studies the complementary use of HeNBs (femtocells 3GPP terminology) to provide broadband services. It is essential to maintain the networks performance with the network densification phenomenon, which brings significant interference problems and consequently more collisions and lost packets. The use of SC-FDE in the downlink of a LTE-A femtocell network - specifically multipacket reception (MPR), with an IB-DFE receiver employing *Multipacket Detection* (MPD) and SIC techniques is proposed. A new telecommunications concept named GC emerged with the increasing environmental concerns. This dissertation shows the performance results of an iterative MPR and proposes a green association algorithm to change the network layout according to the mobile users demands reducing the *Base Station* (BS)'s negative contribution to the network total energy consumption. The overall results show that the technologies employed are a solution to achieve a favorable trade-off between performance and *Energy Efficiency* (EE), responding to the global demands (high data rates) and concerns (low energy consumption and carbon footprint reduction).

Keywords: Long Term Evolution(LTE), Single Carrier with Frequency Domain Equalization (SC-FDE), Iterative Block-Decision Feedback Equalizer (IB-DFE), Home enhanced Node B (HeNB), Successive Interference Cancellation(SIC),Multipacket Reception(MPR), Green Communications (GC) ,

Acronyms

3GPP *3rd Generation Partnership Project*

AP Access Point

ARQ *Automatic Repeat reQuest*

AWGN *Additive White Gaussian Noise*

BER *Bit Error Rate*

BS *Base Station*

CA *Closed Access*

CDMA *Code Division Multiple Access*

CoMP *Coordinated Multipoint*

CP *Cyclic Prefix*

C-Plane *Control Plane*

CSG *Closed Subscriber Group*

DFE *Decision Feedback Equalizer*

DFT *Discrete Fourier Transform*

DIM *Distributed Interference Management*

DL *Downlink*

EDGE *Enhanced Data rates for GSM Evolution*

EE *Energy Efficiency*

eNB *Enhanced Node B*

EPC *Evolved Packet Core*

EPS *Evolved Packet System*

E-UTRAN *Evolved UTRAN*

FD *Frequency Domain*

FDE *Frequency-Domain Equalization*

FFT *Fast Fourier Transform*

FFR *Fractional Frequency Reuse*

GC *Green Communications*

GSM *Global System for Mobile Communications*

HA *Hybrid Access*

HARQ *Hybrid Automatic Repeat reQuest*

HeNB *Home enhanced Node B*

HeNB-GW *Home eNodeB Gateway*

HNet *Heterogeneous Network*

HSDPA *High-Speed Downlink Packet Access*

HSPA *High Speed Packet Access*

HSDPA *High-Speed Uplink Packet Access*

IA *Interference Avoidance*

IB-DFE *Iterative Block-Decision Feedback Equalizer*

IC *Interference Cancellation*

ICI *Inter-Carrier Interference*

IDFT *Inverse Discrete Fourier Transform*

IFFT *Inverse Fast Fourier Transform*

IMT-A *International Mobile Telecommunications-Advanced*

InH *Indoor Hotspot scenario*

IPSec *Internet Protocol Security*

ISI *Inter-Symbol Interference*

ITU *International Telecommunication Union*

ITU-R *International Telecommunication Union Radiocommunication Sector*

LLR *Log-Likelihood Ratio*

LoS *Line-of-Sight propagation*

LTE *Long Term Evolution*

LTE-A *Long Term Evolution Advanced*

MAI *Multi Access Interference*

MC *Multi-Carrier*

MIMO *Multiple-Input and Multiple-Output*

MME *Mobility Management Entity*

MMSE *Minimum Mean Square Error*

MPD *Multipacket Detection*

MPR *Multipacket Reception*

NLoS *Non-Line-of-Sight propagation*

OA *Open Access*

OFDM *Orthogonal Frequency-Division Multiplexing*

OFDMA *Orthogonal Frequency-Division Multiple Access*

OPEX *Operational expenditure*

PAPR *Peak-to-Average Power Ratio*

P-GW *Packet-data Network Gateway*

PER *Packet error rate*

PHY *Physical layer*

PIC *Parallel Interference Cancellation*

PL *Pathloss*

QAM *Quadrature amplitude modulation*

QoS *Quality of Service*

QPSK *Quadrature Phase-Shift Keying*

RF *Radio Frequency*

SAE *System Architecture Evolution*

SC *Single Carrier*

SC-FDE *Single Carrier with Frequency Domain Equalization*

SC-FDMA *Single Carrier Frequency-Division Multiple Access*

SeGW *Security Gateway*

S-GW *Serving Gateway*

SIC *Successive Interference Cancellation*

SINR *Signal-to-Interference-plus-Noise Ratio*

SNR *Signal-to-Noise Ratio*

SON *Self-Organizing Network*

TD *Time Domain*

UE *User Equipment*

UL *Uplink*

UMa *Urban Macro-cell scenario*

UMi *Urban Micro-cell scenario*

UMTS *Universal Mobile Telecommunications System*

U-Plane *User Plane*

UTRAN *Universal Terrestrial Radio Access Network*

ZF *Zero Forcing*

Contents

List of Figures

List of Tables

List of Symbols

B_k	Receiver feedback coefficients
E_b	Average bit energy associated to a given packet transmission
$F_{k,p}$	Receiver Feed-forward coefficients
$H_{k,p}^{(l)}$	Channel frequency response from the pth user, during the lth transmission
N_0	Power spectral density of the noise
$N_k^{(l)}$	The channel noise during the lth transmission
P	Number of transmitting HeNBs
$S_{k,p}$	Data block transmitted by a user p, in the frequency domain
$s_{k,p}$	Data block transmitted by a user p, in the time domain
Th	Throughput
$Y_k^{(l)}$	Received signal, from multiple HeNBs, at the receiver in the frequency domain for a given transmission l
τ_c	Cluster delay
P_c	Cluster power
λ	UE load requirement

Chapter 1

Introduction

In recent years, due to the continuous technology development, operators saw a rapid growth of mobile broadband subscribers as well as of their traffic volume demanded, specially due to the introduction of more advanced mobile devices and real time services [1]. As a consequence of this, there is also an increasing demand for high speed data rate services. Under the partnership of the 3GPP, LTE was developed and proposed to subscribers to fulfill this ambitious task. LTE evolution, known as LTE-A, was the first to meet the *International Mobile Telecommunications-Advanced* (IMT-A) requirements for 4G systems, promising among others [2], peak data rates up to 1 Gbit/s. To achieve the desired hight data rates, LTE-A proposed a set of features such as spectrum flexibility, multi-antenna transmission, scheduling and link adaptation, carrier aggregation, relay nodes, *Heterogeneous Network* (HNet)s and *Coordinated Multipoint* (CoMP), among others [3]. LTE radio access exploit rapid variations in channel quality in order to make more efficient use of available radio resources. This is done in both time and frequency domains using *Orthogonal Frequency-Division Multiplexing* (OFDM) and SC-FDE multiple access versions, known as *Orthogonal Frequency-Division Multiple Access* (OFDMA) and *Single Carrier Frequency-Division Multiple Access* (SC-FDMA), in the *Downlink* (DL) and *Uplink* (UL) respectively. One of the major concerns is the probable lack of capacity due to the rapid and continuous growth of traffic data demands. The concept of HNet was introduced to face this problem, which briefly consists on adding a second layer to the existing network (macro BSs), dedicated to low power BSs [4]. Seen as the most

cost-efficient solution to both service provider and end user , the femtocell BS (or HeNB in 3GPP) terminology deployment became a reality. Femtocell networks use the same *Physical layer* (PHY) technology as macro cellular networks, which means OFDM and SC-FDE multi access versions, serving less users compared to the macro network. Although it enhances the overall network performance, the HNet approach also brings new concerns such as the increase of the interference level [4].

1.1 Motivation

According to the requirements, LTE-A is expected to provide higher data rates. Increasing the BSs transmit power seems to be the logical solution. However, it causes higher interference in the network and consequently reduces the network efficiency (performance). To enhance the network performance/efficiency, the decrease of the cell size, reducing the BSs transmit power, seems to be the solution. This reduction is compensated with an increase in the number of deployed BSs in the network. With the emerge of these low power BSs, known as femtocell base stations or HeNB in 3GPPs terminology, the network layout was redesigned, bringing the UEs and the BSs closer to each other. To take advantage of the low power transmissions, an efficient reception becomes essential to enhance HeNBs coverage range and communication links reliability. In addition, most of the proposed solutions to deal with poor transmission conditions forgot the Energy Efficiency(EE) issue, being typically performance-oriented.

1.2 Objectives and Contributions

LTE-A telecommunication services predict the existence of macro base stations, eNB, and femto base stations HeNB with low power that complements the network's coverage. This dissertation aims to study the complementary use of HeNBs to provide ultra-wideband services. It is assumed that there is a fiber network interlinking the HeNBs, allowing the use of MPR, and switch off techniques. To handle the network densification phenomenon, which brings significant interference problems and consequently more collisions and lost packets, this research work proposes the use of SC-FDE in the downlink of a LTE-A

femtocell network - specifically the use of an IB-DFE receiver employing MPD and SIC techniques. The work is divided in two parts: the first part (chapter 3) analyzes the enhancements achieved with the IB-DFE receiver and MPR technique when multiple HeNBs transmit concurrently. In the second part (chapter 4) it is discussed the appliance of the iterative SIC receiver and MPR technique combined with a switch off technique. The main objective is to achieve the best trade off between performance and energy efficiency, according to the global demands (high data rates) and concerns (low energy consumption and carbon footprint reduction). This work main contributions are :

- It shows the IB-DFE receiver employing MPR technique applicability in the downlink of a LTE-A femtocell based network.
- The development of a green association algorithm, which achieves a trade-off between energy efficiency and performance, changing the network layout according to the mobile users demands.

1.3 Thesis Structure

Chapter 2 presents the LTE networks key characteristics and features. A brief description of LTE evolutionary process is presented in section 2.1.1. The LTE-A network architecture is depicted in section 2.1.2. The DL and UL multi access schemes adopted are discussed in section 2.1.3. Section 2.1.4 addresses the emerging of small cells. Relevance is given in this thesis to a specific type of small cell named femtocell or HeNB, being explained its concept in section 2.2.1, the fundamental changes that it introduce to the existing network architecture in section 2.2.2 and its modus operandi in terms of access modes and spectrum allocation in sections 2.2.3 and 2.2.4 respectively. Section 2.3 addresses the concept of HNets and discussed the associated interference problems and some possible solutions.

Chapter 3 discusses several aspects related to the possible adoption of a single carrier transmission scheme, named SC-FDE, in a downlink of an LTE femtocell based network. Firstly, section 3.1 presents the concept and explains in detail the various types of receivers respectively in sections 3.1.1, 3.1.2 and 3.1.3. The MPR technique, which applies MPD and

SIC approaches, is explained in detailed in section 3.1.4. In section 3.1.5 it is presented the *Packet error rate* (PER) calculation model used in this work. The network interference is characterized in section 3.2. Section 3.3 describes the adopted propagation model, being the detailed explanation of the channel generation process given in section 3.4. Finally, in section 3.5 the performance results regarding to the use of the proposed receiver in the set of chosen simulation scenarios are exhibited and discussed.

Chapter 4 starts with the explanation of the GC concept, concerns and proposed approaches in section 4.1. In section 4.2 it is presented and explained in detail the proposed green algorithm. Finally, in section 4.3 is discussed the performance results in terms of energetic gains, regarding the green algorithm appliance in the definition of a LTE-A femtocell based network layout.

Chapter 2

State of the art

This chapter provides a brief overview of LTE, addressing key topics such as, network architecture, applied multiple access schemes and other relevant issues related to the introduction of the small cells (femtocells) approach.

2.1 LTE (Long Term Evolution)

As a consequence of the technological evolution emerged a new concept of mobile users, more demanding and accustomed to access broadband services everywhere.
Mobile broadband, has become a necessity. The *Global System for Mobile Communications* (GSM) answered to this trend developing new mobile technologies to achieve high quality of services and better performances, such as higher data rates, larger capacity, greater spectral efficiency, packet switched optimized system and cheaper infrastructure.
LTE was a step beyond 3G and towards the 4G and evolved after *Enhanced Data rates for GSM Evolution* (EDGE), *Universal Mobile Telecommunications System* (UMTS), *High Speed Packet Access* (HSPA) and HSPA Evolution, to face users increasing demands and ensure 3GPP's competitive edge over other cellular technologies [5]. The evolution towards LTE began with Release 98 specifying GSM and then continued with Release 99. Release 99 specifies UMTS with *Code Division Multiple Access* (CDMA) air interface. The technology moved to an all-IP network development in Release 4. UMTS networks development moved to HSPA, introduced in 2002 by Release 5 (*High-Speed Downlink Packet Access* (HSDPA)) and Release 6 (*High-Speed Uplink Packet Access* (HSDPA)). The

improvements in mobile technologies went on by HSPA+, which is described in Release 7.

2.1.1 Evolution to LTE-A

The first version of LTE was completed in March 2009 as part of 3GPP Release 8 and just like the majority of the technologies, it went through an evolutionary process. In order to properly respond to increasing operator and end-user expectations, the LTE radio access technology is continuously evolving. In this evolutionary process, releases 9 and 11 were seen as intermediate releases that introduced multi-cast / broadcast functionality and CoMP transmission and reception of BSs respectively.

Releases 10 and 12 were the major steps in this continuous evolution. The first one commonly referred to as LTE-A [6] introduced carrier aggregation, *Multiple-Input and Multiple-Output* (MIMO) evolution up to 8×8 and 4×4 in the DL and UL respectively, relay nodes, small cells and HNets [7][8], allowing LTE to meet IMT-A requirements for 4G systems, such as peak data rates up to 1 Gbit/s, as defined by the *International Telecommunication Union Radiocommunication Sector* (ITU-R)[9].

3GPP's release 12 targets the increasing demand for mobile broadband services and traffic volumes focusing areas like capacity increase, energy savings, cost efficiency, support for diverse application and traffic types, higher user experience/data rate and small cells [10].

2.1.2 Network Architecture

LTE embraces the evolution of the radio access through the *Evolved UTRAN* (E-UTRAN), accompanied by the evolution of non-radio aspects termed *System Architecture Evolution* (SAE), originating the overall architecture termed *Evolved Packet System* (EPS) [11].

The *Evolved Packet Core* (EPC), or EPS core network, is a flat, packet switched all-IP network . Its architecture is divided in two planes: *Control Plane* (C-Plane) and *User Plane* (U-Plane). EPC consists of functional entities including C-Plane nodes such as *Mobility Management Entity* (MME) and U-Plane nodes such as *Serving Gateway* (S-GW) and *Packet-data Network Gateway* (P-GW). The flat and fully distributed radio-access network architecture E-UTRAN [12], as depicted in figure 2.1 , consists of base stations, denoted as enhanced Node B(eNB). The eNBs are responsible for managing multiple cells,

as well as, implement all related radio functions, such as Radio Resource Management, Header compression, security, positioning and connectivity to EPC. The interface X2 enables direct communication between eNBs, supporting mobility, inter-cell interference management and *Self-Organizing Network* (SON) functionalities. S1 connects E-UTRAN and EPC, connecting eNBs to MME and S-GW entities .

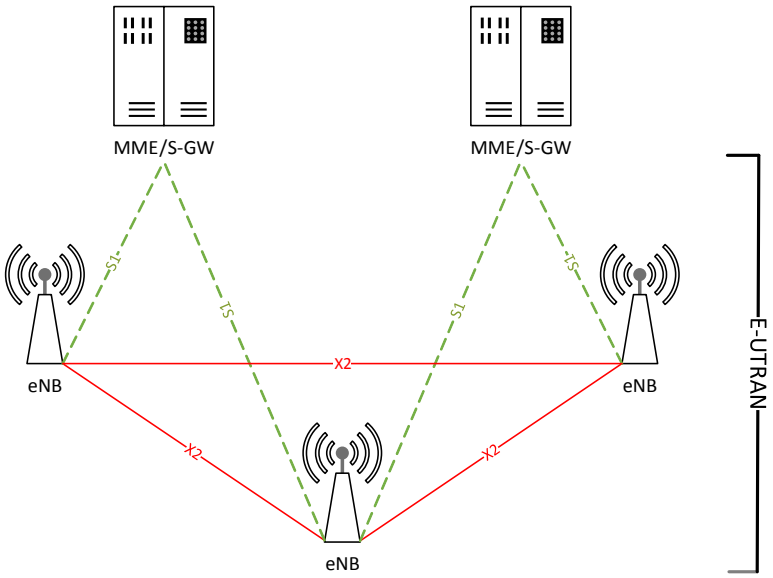

Figure 2.1: LTE Radio Access Network Architecture

2.1.3 Multiple access schemes

The adopted multiple access schemes for DL and UL in LTE are built over OFDM and SC-FDE modulations. This section starts with a brief introduction to OFDM main characteristics, being the SC-FDE explained in detail later in chapter 3.

2.1.3.1 Orthogonal Frequency Division Multiplexing (OFDM)

OFDM is widely used in wideband wireless communications due to the numerous advantages associated to its usage, where the ability to handle severe channel conditions should be highlighted [13]. OFDM is a *Multi-Carrier* (MC) transmission scheme in which a single channel with a certain frequency band uses multiple sub-carriers on adjacent frequencies. In order to maximize spectral efficiency and simultaneously prevent adjacent channel interference or *Inter-Carrier Interference* (ICI), the sub-carriers are orthogonally overlapping (see figure 2.2)[14]. Each subcarrier is modulated with a conventional modu-

lation scheme (e.g. *Quadrature amplitude modulation* (QAM) or *Quadrature Phase-Shift Keying* (QPSK)) at a much lower rate than the original stream, which combined with the use of an efficient implementation of *Discrete Fourier Transform* (DFT), named as *Fast Fourier Transform* (FFT), to simplify and improve the channel equalization [15].

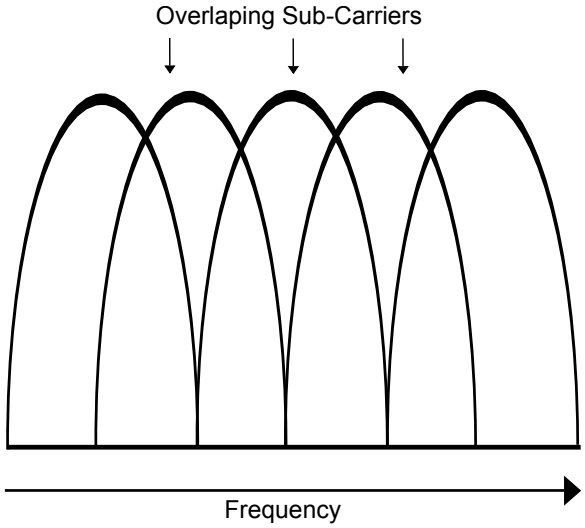

Figure 2.2: OFDM Subcarrier Spectrum

However, communication systems are susceptible to multi-path channel reflections, that leads to delayed copies of the signal and delay spread in transmission, causing *Inter-Symbol Interference* (ISI). To avoid/reduce ISI, the OFDM based transmitter introduces a guard period, known as the *Cyclic Prefix* (CP), between each transmitted data symbol. The CP is a repetition of the last section of the OFDM symbol that is inserted before to its beginning, that does not carry data and its length is chosen in order to be larger than the expected delay spread of the propagation channel, as depicted bellow in figure 2.3.

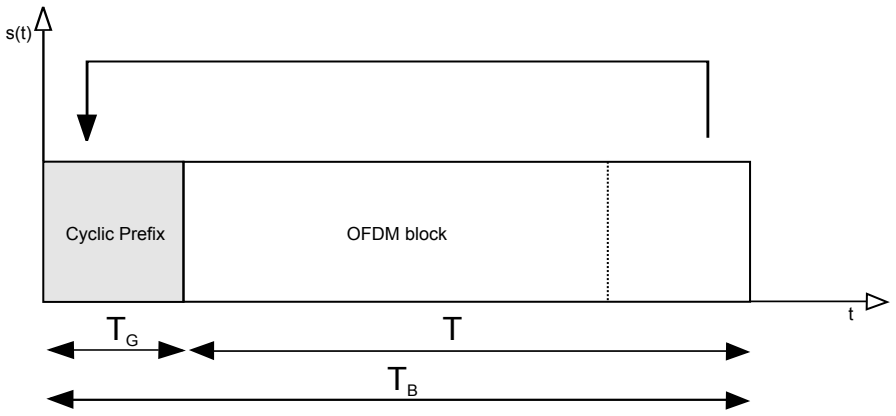

Figure 2.3: OFDM Block Structure with Cyclic Prefix

Similar procedures are applied in the reverse order at the receiver side.A simple OFDM block diagram is shown in figure 2.4.

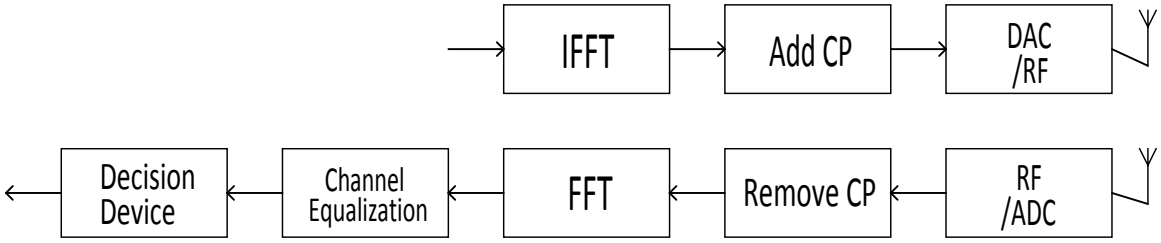

Figure 2.4: Basic OFDM transmitter and receiver block diagram

Although OFDM meets the demands for spectrum flexibility and provides cost-efficient solutions for wide-band wireless communications, it has an enormous drawback (especially to UL communication side): the high *Peak-to-Average Power Ratio* (PAPR), which requires linear transmitter circuitry that can be expensive [16].

2.1.3.2 OFDMA in the downlink

OFDMA was chosen to be the transmission scheme in LTE downlink. It is very similar to OFDM, with the main difference that instead of allocating all the available subcarriers, the BS allocates a subset of carriers to each user in order to accommodate multiple transmissions simultaneously [14]. A block diagram of this multiple access method is depicted in figure 2.5.

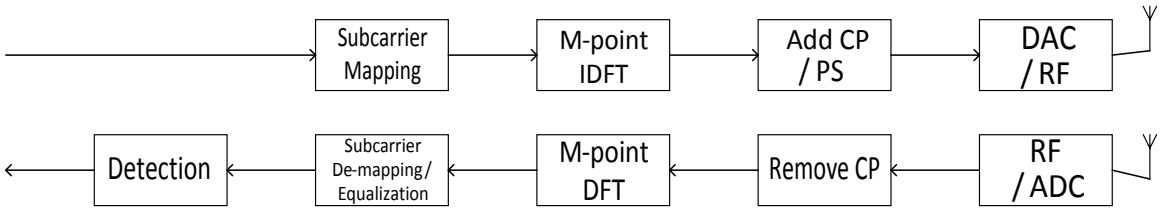

Figure 2.5: Transmitter and receiver structure of OFDMA system.

OFDMA enables the OFDM transmission to benefit from multi-user diversity, based on feedback information about the frequency-selective channel conditions from each user. Adaptive user-to-subcarrier assignment can be performed, enhancing considerably the total system spectral efficiency compared to single-user OFDM systems. OFDMA inherits the advantages but also the drawbacks, from its underlying technology. Since all the frequencies of the subcarriers were generated by one transmitter, in OFDM is relatively

easy to maintain the orthogonality of the subcarriers, whereas in OFDMA, since many users transmit simultaneously, each with their own estimates of the subcarrier frequencies, a frequency offset is inevitable and multiple access interference may occur.

2.1.3.3 SC-FDMA in the uplink

As previously seen in LTE femtocell DL access scheme, the big advantage of OFDMA is its robustness in the presence of multipath signal propagation and its main drawback is the very pronounced envelope fluctuations of the waveform, resulting in a high PAPR in OFDM modulated signals. Signals with a high PAPR require highly linear power amplifiers to avoid excessive inter-modulation distortion. So, to achieve this linearity the amplifiers have to operate with a large back-off from their peak power. Another drawback of OFDMA usage identified for UL transmissions is, the sensitivity to frequency offset (Doppler-Shift). With multiple terminals simultaneous transmissions, different doppler-shifts lead to an orthogonality loss and consequently the introduction of *Multi Access Interference* (MAI). Since power consumption is one of the main concerns of mobile equipment's manufactures, this power inefficiency (measured by the ratio of transmitted power to DC power dissipated) induced/caused by OFDMA usage, that increases the cost of the terminal and reduces battery life, led to the choice of the SC-FDMA as the LTE UL transmission technique [17]. SC-FDMA is the multiple access version of SC-FDE, which is similar to OFDM, in that they both perform channel estimation and equalization in the *Frequency Domain* (FD). The system model for this access method is depicted in figure 2.6.

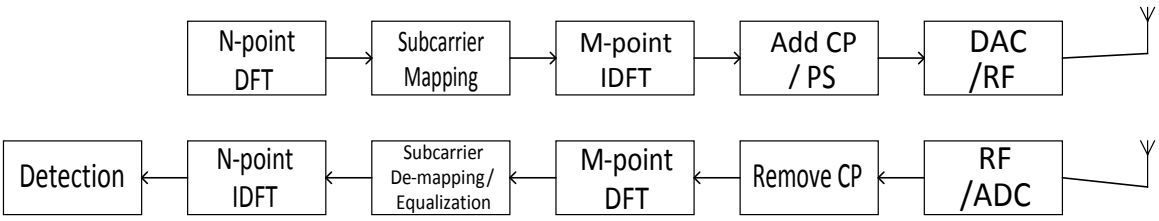

Figure 2.6: Transmitter and receiver structure of SC-FDMA system.

SC-FDMA has two different subcarrier mapping schemes: distributed and localized. In distributed subcarrier mapping scheme, user's data occupy a set of distributed subcarriers achieving frequency diversity. In localized subcarrier mapping scheme, user's data in-

habit a set of consecutive localized subcarriers achieving frequency-selective gain through channel-dependent scheduling. The main differences between OFDMA and SC-FDMA [18]are:

- the DFT block placement in the transmitter side, before symbol to subcarrier mapping, due to the fact that in a *Single Carrier* (SC) transmission each data symbol is transmitted using the entire allocated bandwidth, while in MC transmission only one subcarrier per data symbol is used.
- the *Inverse Discrete Fourier Transform* (IDFT) block placement in the receiver side due to fact that the decision about transmitted bits, contrarily to OFDMA, is done in the *Time Domain* (TD).

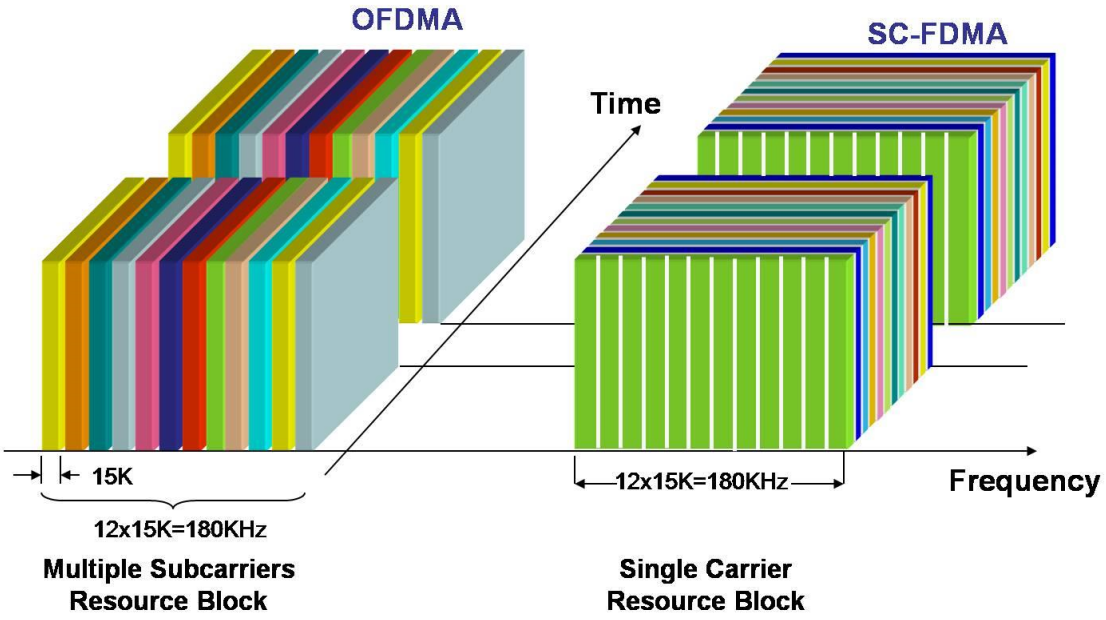

Figure 2.7: OFDMA vs. SC-FDMA

2.1.4 Cell size reduction

As a consequence of the constant technological evolution, the proliferation of high-specification handsets, in particular smart-phones and tablets, is the main reason for the recent mobile users increasing demand for traffic data [19]. As aforementioned in section 2.1, since LTE Release 10, network densification using small cells is a main feature in 3GPP evolutionary

process. This network densification can be achieved with the deployment of complementary low-power BS nodes under the coverage of an existing macro BSs node layer. In such a heterogeneous deployment, low-power nodes bring transmitters and receivers closer to each other providing more spectrally efficient links. Therefore more spatial reuse, higher traffic capacity and end-user throughput (e.g. indoor and outdoor hotspots) is achieved [1], while the macro layer provides wide area coverage. Unlike the high installation and maintenance (infrastructural) cost(s) of macro stations, these low-power nodes constitute a cost-efficient solution to eliminate coverage holes in the network. Types of small cells include femtocells, picocells, metrocells and microcells, broadly increasing in size from femtocells to microcells . Recently, in order to exploit the aforementioned key advantages of small-cells in outdoor high-traffic environments, it is emerging a new concept of macro-assisted small cells, termed Phantom Cell [20].

2.2 LTE Femtocells

As mentioned above in section 2.1.4, small cells are seen as the most promising solution to respond to the increasing mobile communications demands. Comparing all employed techniques to increase mobile networks coverage and capacity (e.g. distributed antenna systems and microcells), femtocells seem to be the most cost-efficient solution to both, service provider and end user.

2.2.1 Concept

The femtocell base station, or HeNB in 3GPP terminology, is a small Access Point (AP) or BS, commonly consumer-deployed, connected via broadband connection or optical fiber technology to the operator's core network. Femtocells small size nature introduces some unpredictability in their deployment. They can be seen as non-static base stations and their deployment is done according users necessities. The lower transmit power reduced end-user distance deployment and the lower number of users served are seen as the main aspects to the power and spectral efficiency and capacity benefits of HeNBs [1]. These promising small base stations are almost total configurable in terms of transmit power and modus operandi. Spectrum allocation, transmission power and operation mode are

the most relevant aspects in terms of femtocells interference level management, affecting its performance and efficiency (discussion is bellow in sections 2.2.3 and 2.2.4).
Femtocell networks use the same physical layer technology as macro cellular networks, which mean OFDMA in the DL and SC-FDMA in the UL to provide, though limited by the backhaul connection, the desired higher data rates and improvement in terms of *Quality of Service* (QoS) to the mobile users [21].

2.2.2 Architecture E-UTRAN

As the inclusion of femtocell technology is essential for the LTE evolutionary process, it was necessary to develop the standardized LTE femtocell network architecture taking in account LTE SAE requirements. The deployment of femtocells introduces a new network architecture concept termed a two-layer or two-tier network, composed of two clearly separated layers: the macro cell layer and the femtocell layer (introduced bellow in section 2.3). The femtocell network architecture has been defined to allow maximum flexibility and scalability, to ensure that the deployment can be easily incorporated into the existing structures. It was kept in the flattest manner due to the adoption of an all-IP networks in LTE access network architecture (see section 2.1.3). Interface S1 links E-UTRAN (HeNBs) to EPC and X2 interface is responsible for the communication and information exchange between HeNBs (since Rel-9 or later HeNB implementations). HeNB supported functions and procedures are the same as eNB ones (section 2.1.2), but some modifications were made to the conventional macro cellular networks topology. The main difference is the possible inclusion of a new interface, named *Home eNodeB Gateway* (HeNB-GW), between HeNBs and EPC that leads to a logical division in S1 interface: S1-MME to carry control plane information and S1-U for data plane. The HeNB-GW inclusion in the network architecture is previously referred as a possibility because according to 3GPP technical specifications to HeNB architecture [22] there are three possible variants of HeNB E-UTRAN architecture: without HeNB-GW, with dedicated HeNB-GW and with HeNB-GW for C-Plane.

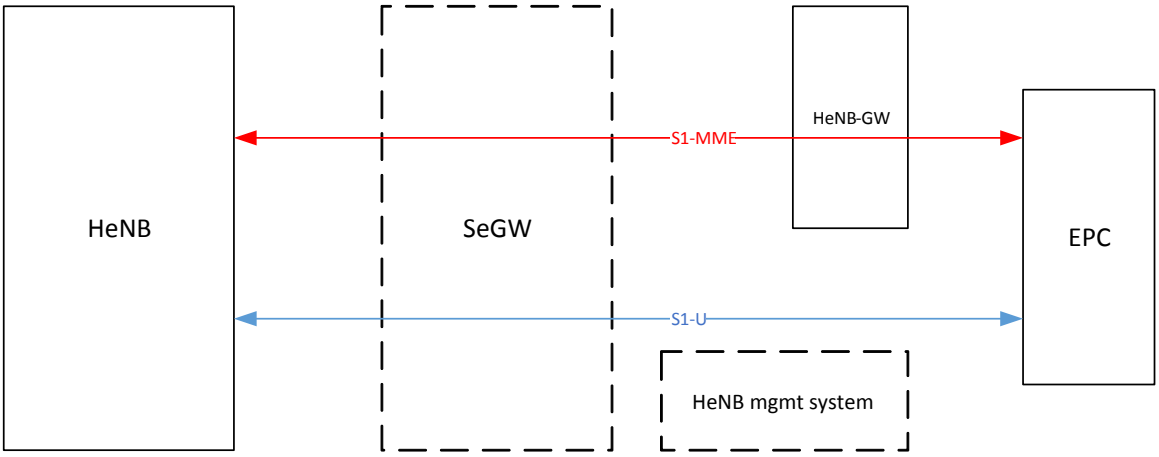

Figure 2.8: LTE femtocell Radio Access Network Architecture

When present, HeNB-GW serves as a concentrator for the C-Plane, specifically the S1-MME interface and in a manner that mobility issues would not require inter-MME handovers. Besides, it may terminate the U-Plane towards the HeNB and S-GW (S1-U) providing support for U-Plane multiplexing, enhancing systems with limited bandwidth links. The communication between the HeNB and MME/S-GW or HeNB-GW/S-GW is secured by the mandatory *Security Gateway* (SeGW) function. The SeGW establishes and manages all *Internet Protocol Security* (IPSec) tunnels that each HeNB needs to ensure the integrity of data exchanged with the network. SeGW can be implemented either as a separate physical entity or co-located with an existing entity such as HeNB-GW.

2.2.3 Access modes

Femtocells can support a limited number of users, so it is important to define the set of users that are authorized to use each HeNB resources, in order words to define the access mode. HeNBs can be configured to operate in one of three available distinct modes[23]: *Open Access* (OA), *Closed Access* (CA) and *Hybrid Access* (HA).

- **OA mode -** allows all users to connect to HeNB, usually applied in public places such as airports.
- **CA mode -** only a restrict set of users is allowed to connect to HeNB. The set of authorized users is saved in a list, termed, *Closed Subscriber Group* (CSG). It is usually applied in home environments.

- **HA mode -** HeNB provides services to its associated CSG members and to non-CSG members, i.e., any UE may access the femtocell (with limited amount of HeNB resources) but preference would be given to those UEs which subscribed to the femtocell. It is usually applied in enterprise environments.

2.2.4 Spectrum allocation

There are two possibilities to deploy femtocells in cellular network spectrum: dedicated channel and shared channel. In dedicated channel deployment, a specific channel is allocated for the femtocell network, which is not used by the macrocell; on the other hand, in shared or co-channel deployment the two layers share all channels i.e. the totality of the available spectrum. Due to the high cost and scarcity of spectrum, operators prefer co-channel realization that increases the overall capacity and enhances spectral efficiency, but causes several interference problems that must be dealt [24].

2.3 Two tier network

As previous referred the deployment of small, low power BSs leads to the redesign of the cellular network, dividing it into two main layers, as shown in figure 2.9: macro cellular layer and femto cellular layer. Despite the numerous advantages in terms of capacity, coverage and overall system quality, it also brings some problems/drawbacks and challenges, specifically in terms of interference .

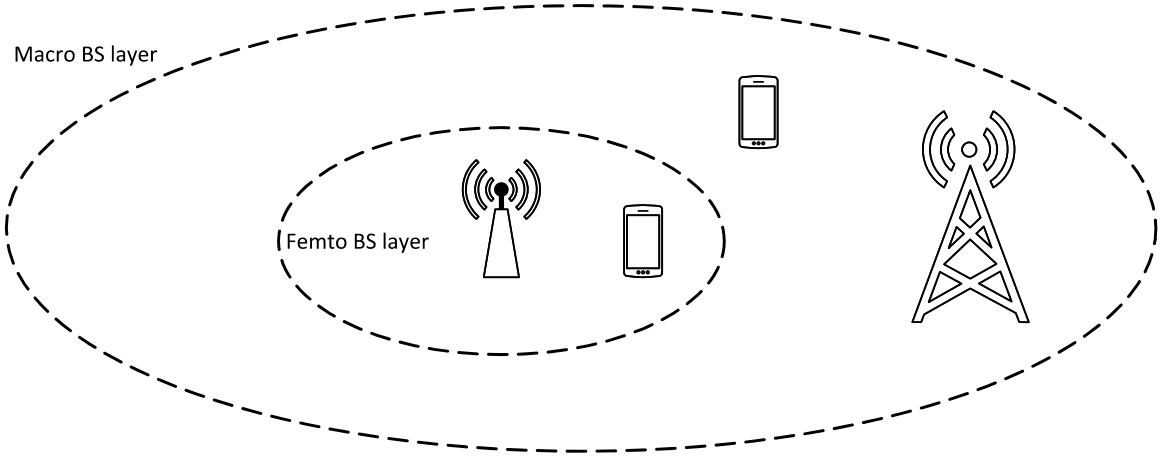

Figure 2.9: Two layer network

2.3.1 Interference challenges

To achieve high data rates, the received signal must have a high SINR, depicted in equation 2.1, meaning that each transmitter should not cause significant interference to base station users. It is essential to maintain or enhance network capacity level.

$$SINR = \frac{S}{I + N} \tag{2.1}$$

where S, I and N represent the desired signal, the interference signal and the noise, respectively. When I and N have Gaussian distributions, the SINR influence can be seen applying the channel capacity concept to an *Additive White Gaussian Noise* (AWGN) channel with B Hz bandwidth and SINR, known as the Shannon-Hartley theorem:

$$C = B \times \log_2 (1 + SINR) \tag{2.2}$$

The interference impact in the overall network performance depends on the adopted air interface technology, such as the OFDMA applied in the downlink of LTE systems. In order to guarantee the required QoS to eNB users, HeNB available spectrum (bandwidth) is reduced, increasing the odds of occurring co-tier interference at the femtocell network (explained above in section 2.3.1.1). The throughput of the network significantly decreases with all types of interference. Severe interference problems lead to zones where the QoS degrades significantly, termed Dead Zones. Two-Tier network design equally leads to a division in two types of interference: Co-Tier and Cross-Tier interferences.

2.3.1.1 Co-tier interference

Co-Tier type refers to the interference caused by elements from the same network layer (e.g. Interference between HeNBs) [25]. HeNBs are low power base stations, with reduced coverage radius, so they are deployed close to users, possibly leading to co-tier interference problems, for example, in residential or in enterprise environments, due their dense deployment. To establish a communication link, the SINR value should be above a certain threshold defined by the used air interface technology taking in account the QoS requirements. When it is not possible to establish the link, the place has no coverage and

usually is termed as “coverage hole”. This is even more frequent / worrying when HeNBs are working in CA mode (creating wider un-coverage areas). Co-tier interference type is equally divided per communication direction, which means per DL or UL. In the UL side Co-Tier interference is caused by femto UE that act as source of interference to neighbor HeNBs. OFDMA femtocells may avoid this type of interference due to the OFDMA division of the spectrum in sub-channels. The BS senses sub-channels conditions. When an UE requires a certain number of sub-channels according to desired QoS, the HeNB allocates sub-channels subject to lower level of interference. The DL Co-Tier interference is caused by a HeNB that acts as source of interference to neighbor femto UEs. This is very common due to the closed distance and dense deployment of HeNBs. Sometimes a simple wall cannot attenuate sufficiently the undesired signals from other BSs. Windows can be a concern too. OFDMA femtocells dynamically sense the air interface and allocate the sub-channels according to sensing results, achieving minimum interference and maximum capacity. 3GPP recommends the use of adaptive power control techniques at HeNBs (especially in CA mode when the serving BS has less power than the interfering one).

2.3.1.2 Cross-tier interference

Cross-tier is the type of interference caused by network elements from a different tier or layer. (e.g. interference between HeNBs and eNBs and vice versa). Again, as in Co-Tier type, this problem is more severe in the presence of CA mode femtocells. This type of interference can be avoided if dedicated spectrum is used for the different layer elements (spectrum splitting), but as already referred, it is a less efficient technique in terms of resources and costs. It can also suffer interference if the bands were adjacent to each other in the frequency domain (adjacent channel interference). In OFDMA systems the femto UE can act as a source of interference to macro BS (eNB) when the femtocell is placed /located /deployed near the eNB, because if femto UE is transmitting with high power in certain sub-channels, those sub-channels become unusable for macro BS, reducing the overall efficiency. The solution is to restrict the femto UE transmission power. Another type is when a macro UE acts as a source of interference to a femto BS. HeNB are normally isolated but due to low wall penetration losses, interference may happen outdoor. Here UE

is transmitting with high power due to being far away from the macro BS, so the HeNB should allocate different sub-channels in order to avoid interference. In the DL, cross-tier interference can be caused by a HeNB close to a macro UE. If the femto BS is working in CA mode, the area around the HeNB becomes a dead-zone or hole in macro coverage. If HeNB was deployed close to eNB, the femtocell coverage area would be reduced due to the interfering signal from the macro BS. Coverage is guaranteed only very near to the femto BS. In OFDMA the DL interference management is mostly dependent on the sub channels allocation [26].

2.3.1.3 Overcoming challenges

The adoption of an efficient interference management scheme leads to a reduction, mitigation or in the best scenario elimination of co and cross types of interference and consequently to an enhancement in the overall network throughput. Several OFDMA femtocells interference management techniques were mentioned and explained in [27]. They are split in three main sections: *Interference Cancellation* (IC), *Interference Avoidance* (IA) and *Distributed Interference Management* (DIM).

On this thesis context, more relevance is given to an IC technique named SIC and to an IA technique named spectrum splitting. IC schemes decode desired information, using along channel estimates to cancel the interference. They require the complete knowledge of the interfering signal's characteristics and an antenna array at the receiver side, making this techniques more suitable to apply in the UL communication and introducing the inherent extra complexity to the BSs. Extensively used in wireless communications, SIC consists in the detection and decoding of one signal per iteration, using the decoded bits from the previous detected signal to cancel it from the combine signal in the next iteration, in order to recover multiple packets . This technique has a complexity and latency proportional to the number of desired signals [28]. For example, when two transmitters share one receiver the common capacity is given by

$$C = \max\left(\left(B \times \log_2\left(1 + \frac{S_1}{N}\right)\right), \left(B \times \log_2\left(1 + \frac{S_2}{N}\right)\right)\right), \tag{2.3}$$

where S_1 and S_2 are the signals of transmitter 1 and 2 respectively.

When employed, SIC capacity gain is observable in [29]:

$$C = B \times \log_2 \left(1 + \frac{S_1 + S_2}{N}\right). \tag{2.4}$$

The spectrum splitting or allocation consists in a set of different approaches that can be adopted to manage OFDM sub-channels. In the dedicated spectrum approach, the licensed spectrum is divided in two parts: one for each layer. It completely eliminates cross-tier interference but it is inefficient in terms of spectrum reuse and cannot avoid ICI and MAI caused by lack of synchronization and orthogonality, especially in dense femtocell deployments. ICI is a major problem in LTE-based systems. Usually mobile operators prefer using a co-channel approach [26], which means that all the available spectrum is used by both layers, increasing the spectral efficiency but also the interference concerns, especially ICI. One approach for reducing ICI from neighboring eNBs and HeNBs is to use enhanced frequency reuse techniques, such as *Fractional Frequency Reuse* (FFR), where only the sub channels that are not used by macrocell, are allocated to femtocell BSs. This last approach is included in a set of proposed solutions [30] based on partial spectrum allocation.

Chapter 3

SC-FDE in the downlink

Block transmission schemes combined with frequency domain processing, such as OFDM, proved to be the most effective solution to support high rate transmissions over severe time dispersive channels. Although, present an impressive tradeoff between performance and processing complexity, OFDM has one considerable drawback: the high envelope fluctuation of frequency domain data blocks. This high range of amplitude in the given signal power, measure by the PAPR, appears as a result of high bandwidth demands, due to transmitter power amplifier nonlinearities and leads to the power inefficiency in the *Radio Frequency* (RF) section of the transmitter. Since the power efficiency became a more relevant issue in mobile communications, a crescent interest in SC modulation methods emerged, which when combined with FDE presents a similar favorable trade-off (performance/low processing complexity) and considerable lower envelope fluctuations than OFDM.

3.1 SC-FDE receiver

In a SC system the signal is transmitted over a single carrier using a conventional modulation scheme such as QAM or QPSK, at a high bit rate. A serious problem to serial data transmissions is the ISI that can be seen as a signal distortion, in which one symbol interferes with subsequent symbols, introducing errors in the decision device at the receiver output, making the communication less reliable. This type of interference is usually associated to negative, multi-path propagation or the inherent non-linear frequency

channel response effects. Thus, an efficient equalization, i.e. the compensation of the distortion caused by channel frequency selectivity becomes essential. In SC-FDE systems a nonlinear equalizer is implemented in FD employing FFT and the CP technique (previously explained in section 2.1.3.1), achieving similar performances compared to OFDM with lower complexity, especially on channels with severe delay spread [31].

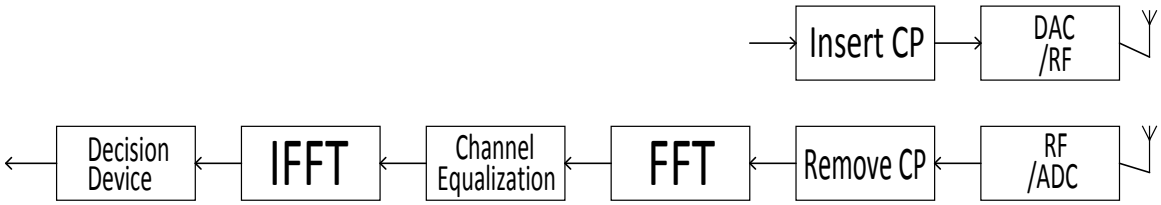

Figure 3.1: Basic SC-FDE transmitter and receiver block diagram

The low PAPR nature of the SC-FDE systems allows an efficient power amplification with non linear amplifiers [32]. SC-FDE systems present a good performance, being substantially more efficient in terms of power consumption than OFDM systems due to the reduced PAPR. Unlike OFDM systems, in which the decision about the transmitted bits is done in the FD, in SC-FDE systems the decision is performed in the TD, which leads to the inclusion of the IDFT block at the receiver side as shown in figure 3.1.

3.1.1 Linear receiver

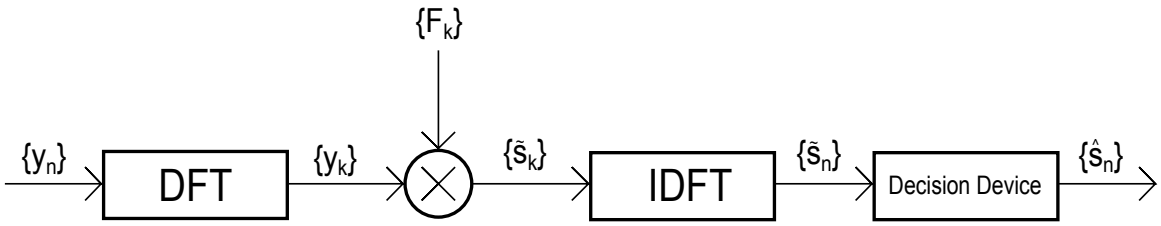

Figure 3.2: SC-FDE receiver structure block diagram

A SC-FDE receiver structure is depicted in fig. 3.2, where the received signal is sampled and its CP removed, resulting in TD samples $\{y_n; n = 0, 1, ..., N-1\}$ which after a N-sized DFT, results in the corresponding FD block $\{Y_k; k = 0, 1, ..., N-1\}$, given by

$$Y_k = H_k S_k + N_k; k = 0, 1, ..., N-1 \tag{3.1}$$

where H_k denotes the overall channel frequency response for the k^{th} frequency of the block and N_k represents channel noise term in frequency-domain. To cope with dispersive channel effects, FDE is employed and it output, frequency-domain samples $\left\{\tilde{S}_k; k = 0, 1, ..., N-1\right\}$ are given by

$$\tilde{S}_k = F_k Y_k, \tag{3.2}$$

where the set of coefficients $\{F_k; k = 0, 1, ..., N-1\}$ denotes the feedfoward FDE coefficients. To avoid the sub-channels noise enhancement and consequently SNR degradation, that usually occurs when an *Zero Forcing* (ZF) equalizer is used, it was employed the *Minimum Mean Square Error* (MMSE) optimization criteria instead. MMSE minimize both effects of ISI and channel noise enhancement [33]. The F_k applied is

$$F_k = \frac{H_k^*}{\alpha + |H_k|^2}, \tag{3.3}$$

with the noise-dependent term, α, that avoids noise enhancement effects for low values of frequency response H_k, denoted as the inverse of SNR value, more specifically given by the ratio,

$$\frac{E[|N_k|^2]}{E[|S_k|^2]} = \frac{\sigma_N^2}{\sigma_S^2}, \tag{3.4}$$

where σ_N^2 represents the variance of the real and imaginary parts of the channel noise components $\{N_k; k = 0, 1, ..., N-1\}$ and σ_S^2 denotes the variance of both real and imaginary parts of the data samples components $\{S_k; k = 0, 1, ..., N-1\}$.

3.1.2 Iterative receiver - IB-DFE

SC-FDE performance can be further improved if an IB-DFE is used . In comparison to linear equalizers, such as the previous described FDE, the nonlinear *Decision Feedback Equalizer* (DFE), as proposed in [34], provides better performances, keeping or enhancing the favorable tradeoff between performance and complexity. Non linear equalizers based in hybrid-solutions were also proposed, where time and frequency domain filters were implemented in the feedback and forward operations respectively [34]. Although this hybrid-DFE approach presents better performances than linear FDE, the number of "feedback" taps increases with the number of rays leading to problems related to error

propagation. IB-DFE approach is a promising iterative technique for SC-FDE, proposed in [35], where the feedback and forward operations are both implemented in FD, presenting low noise enhancement and block reliability on the feedback loop similar to turbo FDE schemes with small error propagation associated [35]. If the estimates of the transmitted block are reliable, the feedback filter can be employed to eliminate the residual ISI. An IB-DFE receiver structure is depicted in figure 3.3,

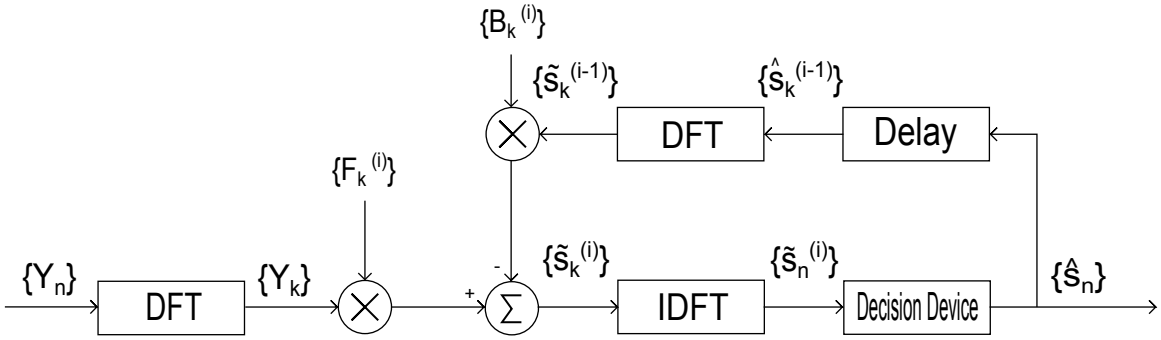

Figure 3.3: IB-DFE with hard-decisions receiver structure

where for the i^{th} iteration, the DFE output block samples are given by

$$\tilde{S_k}^{(i)} = F_k^{(i)} Y_k - B_k^{(i)} \hat{S_k}^{(i-1)}, \tag{3.5}$$

with

$$Y_k = S_k H_k + N_k, \tag{3.6}$$

where $\left\{F_k^{(i)}; k = 0, 1, ..., N-1\right\}$ and $\left\{B_k^{(i)}; k = 0, 1, ..., N-1\right\}$ are the feedfoward and feedback coefficients respectively. $\left\{\hat{S_k}^{(i-1)}; k = 0, 1, ..., N-1\right\}$ represents a DFT of the estimated (hard-decision) block of the previous DFE iteration transmitted block $\{s_n; n = 0, 1, ..., N-1\}$. Both feedfoward ($F_k^{(i)}$) and feedback ($B_k^{(i)}$) IB-DFE coefficients, are chosen to maximize themSINR, which is seen as the IB-DFE optimization.

$$SINR^{(i)} = \frac{\left|\gamma^{(i)}\right|^2 E\left[|S_k|^2\right]}{E\left[|\varepsilon_k^{(i)}|^2\right]} \tag{3.7}$$

Considering a hard decision IB-DFE, the optimum $B_k^{(i)}$ and $F_k^{(i)}$, respectively, are

$$B_k^{(i)} = \rho^{(i-1)}(F_k^{(i)}H_k - \gamma^{(i)}) \tag{3.8}$$

and

$$F_k^{(i)} = \frac{\kappa^{(i)}H_k^*}{\alpha + (1-(\rho^{(i-1)})^2)|H_k|^2} \tag{3.9}$$

where $\kappa^{(i)}$ is chosen to assure that the "mean value of the channel"

$$\gamma^{(i)} = \frac{1}{N}\sum_{k=0}^{N-1} F_k^{(i)}H_k = 1. \tag{3.10}$$

The α coefficient is given by equation 3.4 and the correlation coefficient from the previous iteration $\rho^{(i-1)}$, which is determinant to ensure a good receiver performance since it supplies a block-wise reliable measure of the estimates employed in feedback loop. It is defined as

$$\rho^{(i-1)} = \frac{E[\hat{s_n}^{(i-1)}s_n^*]}{E[|s_n|^2]} = \frac{E[\hat{S_k}^{(i-1)}S_k^*]}{E[|S_k|^2]}, \tag{3.11}$$

where $\hat{s_n}^{(i-1)}$ represents the data estimates associated to the previous iteration and $\hat{S_k}^{(i-1)}$ its associated DFT result. In order to reduce error propagation associated problems hard-decisions per block and overall block reliability are considered in the feedback loop. Therefore, for the first iteration the IB-DFE receiver is simply reduced to a linear FDE.

3.1.3 IB-DFE with soft decisions

As depicted in figure 3.5, the IB-DFE performance can be improved with the use of "soft decisions", $\bar{s}_n^{(i)}$, instead of "hard decisions", $\hat{s}_n^{(i)}$, meaning the use of symbol averages instead of blockwise averages. So applying the soft estimation, the equation (3.5) can be rewritten as

$$\tilde{S_k}^{(i)} = F_k^{(i)}Y_k - B_k^{(i)}\bar{S_k}^{(i-1)}, \tag{3.12}$$

in which the soft decision estimates from the previous iteration, $\bar{S_k}^{(i-1)}$, i.e. the overall block average of $S_k{}^{(i-1)}$ at the 'DFE output', is given by

$$\bar{S_k}^{(i-1)} = \rho^{(i-1)}\hat{S_k}^{(i-1)}, \tag{3.13}$$

where $\rho^{(i-1)}$ represents the block wise reliability of the hard decision estimates $\hat{S}_k^{(i-1)}$.

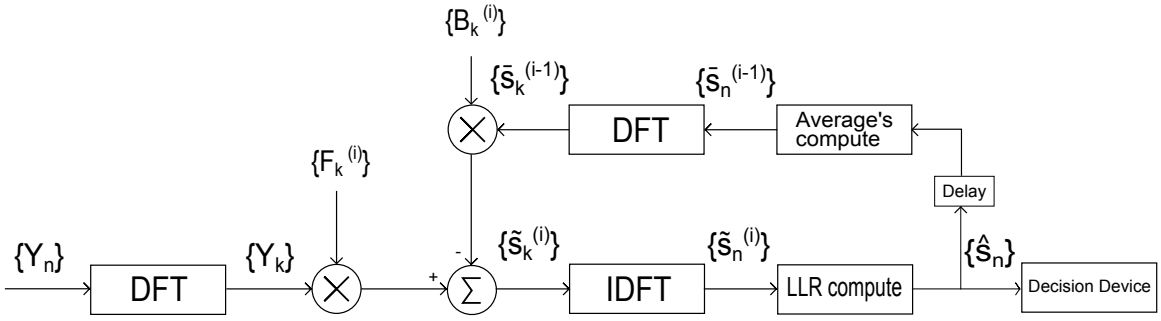

Figure 3.4: IB-DFE with soft-decisions receiver structure

The receiver structure for IB-DFE with "soft-decisions" is depicted in figure 3.4, being the used feedforward coefficients ($F_k^{(i)}$) given by equation 3.9. At the DFE output, the TD samples ($\tilde{s}_n^{(i)}$) are de-mapped into the corresponding bits by means of computing the *Log-Likelihood Ratio* (LLR) of each bit of the transmitted symbols. Assuming that the transmitted symbols are selected from a QPSK constellation with gray mapping, then $s_n = s_n^I + j s_n^Q = \pm 1 \pm j$ in which s_n^I and s_n^Q denote the real and imaginary parts of s_n, respectively.

Thus, the LLRs of "in-phase bit" and "quadrature bit", associated to s_n, are

$$L_n^{I(i)} = \frac{2\tilde{s}_n^{I(i)}}{\sigma_i^2}, \tag{3.14}$$

and

$$L_n^{Q(i)} = \frac{2\tilde{s}_n^{Q(i)}}{\sigma_i^2}, \tag{3.15}$$

respectively, with $\left\{\tilde{s}_n^{(i)}; n = 0, 1, ..., N-1\right\} = \text{IDFT}\left\{\tilde{S}_k^{(i)}; k = 0, 1, ..., N-1\right\}$.

The variance σ^2 is given by

$$\sigma_i^2 = \frac{1}{2} E\left[|s_n - \tilde{s}_n^{(i)}|^2\right] \approx \frac{1}{2N} \sum_{n=0}^{N-1} |\hat{s}_n^{(i)} - \tilde{s}_n^{(i)}|^2, \tag{3.16}$$

where $\hat{s}_n = \pm 1 \pm j$ are the hard-decisions associated to $\tilde{s}_n$.

Therefore, the average symbol values conditioned to the DFE output $\left\{\bar{s}_n^{(i)}; n = 0, 1, ..., N-1\right\}$, are

$$\bar{s}_n^{(i)} = \tanh\left(\tfrac{L_n^{I(i)}}{2}\right) + j \tanh\left(\tfrac{L_n^{Q(i)}}{2}\right) = \rho_n^I \hat{s_n}^I + j \rho_n^Q \hat{s_n}^Q \tag{3.17}$$

with ρ_n^I, ρ_n^Q denoting the reliabilities related to in-phase and quadrature bit of the n^{th} symbol, respectively.

Consequently, the correlation coefficient that will be employed to compute the optimal feedforward coefficients in order to minimize the SINR for a QPSK constellation, is

$$\rho^{(i)} = \frac{1}{2N} \sum_{n=0}^{N-1} \left(\rho_n^{I(i)} + \rho_n^{Q(i)} \right) \tag{3.18}$$

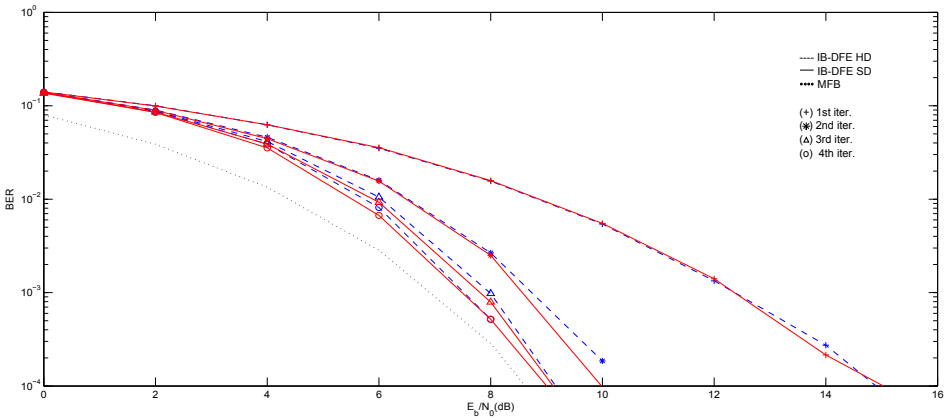

Figure 3.5: IB-DFE with hard and soft decisions performances with QPSK constellation

3.1.4 Multipacket Reception

Although all efforts to achieve perfect transmission links, it has proved to be complicated, due to the unpredictability of the factors involved in the transmission process such as noise interference level and collisions, which cause poor transmission conditions and consequently the loss of the transmitted packets. This is even more critical in a scenario of multiple and simultaneous transmissions to a common receiver, where the interference level and the number of collisions increase. One of the major problems is the fact that transmitters tend to increase their transmit power to overcome the bad transmission conditions, such as high noise level. Several techniques were proposed to cope with lost packet problem, namely the MPD employed in this study in a reception technique denoted by MPR. MPR denotes the capability of simultaneous decoding of more than one packet from multiple concurrent transmissions [36]. As depicted in figure 3.6, the suboptimal MPD techniques can be categorized in two types: linear and non-linear (or subtractive

interference) detection techniques.

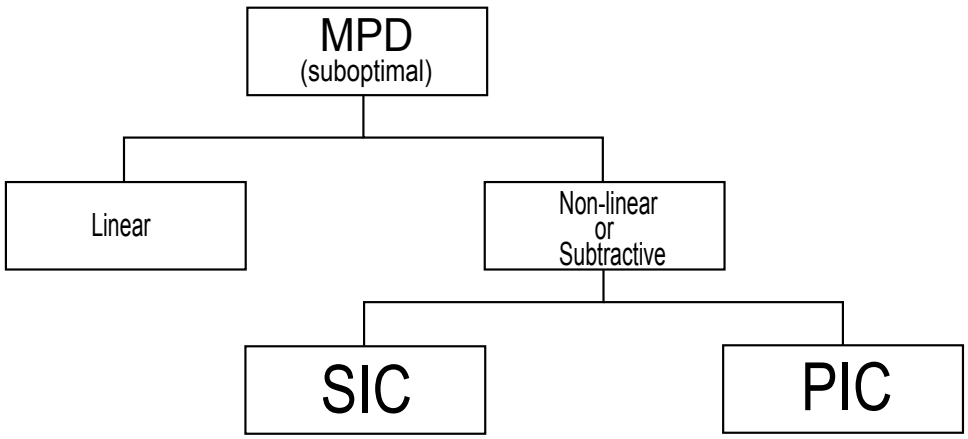

Figure 3.6: Suboptimal MPD techniques

The Decorrelating and MMSE are the most popular multiuser linear detectors, in which a linear mapping to the soft output of a conventional detector is applied, in order to reduce the MAI. However, there are fundamental differences between these two linear detectors. Whereas the Decorrelating detector (highly analogous to ZF equalizer) attempts to completely eliminate the MAI from all users, applying the inverse correlation matrix at the match filter bank output, the MMSE instead tries to minimize the square of residual noise plus interference applying a modified inverse correlation matrix at the match filter bank output, obtaining better results than the Decorrelating detector which often results in an unacceptable noise enhancement.

Subtractive interference or IC techniques require reliable received signal estimation, meaning an accurate description of what was transmitted as well as the channel effects in that transmission. These techniques can be organized in two categories: the use of a parallel *Parallel Interference Cancellation* (PIC) or serial/successive SIC approach in the packet detection process. As the name suggest, SIC employs a serial approach i.e. just one packet is detected per stage, according to their power at the receiver, starting with the powerful one and so on. The packet is regenerated between the soft estimation of each transmitted packet. Afterwards the regenerated packet is subtracted from the composite received signal, allowing the subsequent packet detection to experience less MAI. On the other hand in PIC, approach the packets are detected in parallel, meaning all packets are simultaneously detected and the resulting estimation is used to cancel some interference

to the composite received signal. Although PIC presents a lower latency, it usually has a higher level of complexity compared to SIC approach which has a complexity and latency proportional to the number of packets [28].

There are several MPD approaches. In this study a MPD technique based on time diversity [32] was considered, in which all transmitters involved in a collision (P), transmit several copies of their packets under slightly modified transmission conditions, in order to allow their separation at the receiver. So, the received content at the UE $\{Y_k; k = 0, 1, ..., N-1\}$ is

$$Y_k^{(L)} = H_{k,P}^{(L)} S_{k,P} + N_k^{(L)}, \tag{3.19}$$

or the expanded expression

$$\begin{bmatrix} Y_k^{(1)} \\ \vdots \\ Y_k^{(L)} \end{bmatrix} = \begin{bmatrix} H_{k,1}^{(1)} & \cdots & H_{k,P}^{(1)} \\ \vdots & \ddots & \vdots \\ H_{k,1}^{(L)} & \cdots & H_{k,P}^{(L)} \end{bmatrix} \begin{bmatrix} S_{k,1} \\ \vdots \\ S_{k,P} \end{bmatrix} + \begin{bmatrix} N_k^{(1)} \\ \vdots \\ N_k^{(L)} \end{bmatrix}. \tag{3.20}$$

where L denotes the number of required retransmissions, meaning the temporal diversity order and P represents the number of BSs involved in the transmission.

As aforementioned in section 3.1.2, both feedforward and feedback filters are implemented in FD, being, for each iteration, the first responsible for partially equalizing the interference and the second for the partial removal of the residual interference.

The iterative process gradually increases the reliability of the detected packet. At the first iteration the feedback coefficients are zero and the equalizer is a linear MMSE equalizer. In the iterative SIC receiver applied [37], each iteration consists in NP detection stages (one stage for each collision) as depicted in figure 3.7.

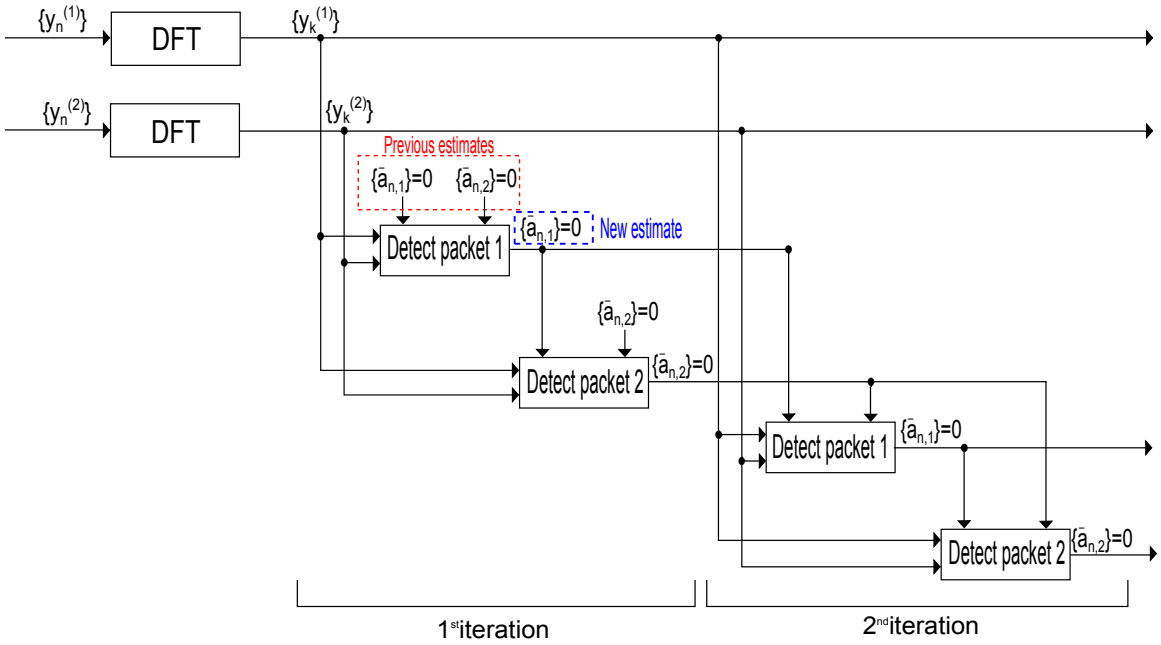

Figure 3.7: Iterative SIC receiver detecting two packets involved in a collision

When detecting a packet its residual ISI is removed, as well as the residual interference from other packets. The receiver is composed by NP FD feedfoward filters, one for each retransmission l and NP FD feedback filters one for each packet p. This SIC receiver uses the average values associated to a given packet $\bar{s}_{n,p}$, conditioned to DFE output given by

$$\tilde{S}_{k,p} = \sum_{l=1}^{NP} F_{k,p}^{(l)} Y_k^{(l)} - \sum_{p'=1}^{P} B_{k,p}^{(p')} \bar{S}_{k,p'} \tag{3.21}$$

where the average values $\bar{S}_{k,p'}$ are computed as previously explained in section 3.1.3, so the optimum feedfoward that minimize SINR for a given packet and iteration are

$$F_{k,p}^{(l)} = \frac{\breve{F}_{k,p}^{(l)}}{\gamma_p} \tag{3.22}$$

with

$$\gamma_p = \frac{1}{N} \sum_{k=0}^{N-1} \sum_{l=1}^{NP} \breve{F}_{k,p}^{(l)} H_{k,p}^{(l)} \tag{3.23}$$

being $\breve{F}_{k,p}^{(l)}$ computed from

$$(1-\rho_p^2)H_{k,p}^{(l)*}\sum_{l'=1}^{NP}\breve{F}_{k,p}^{(l)}\breve{F}_{k,p}^{(l)}+\sum_{p'\neq p}(1-\rho_p'^2)H_{k,p'}^{(l)*}\sum_{l'=1}^{NP}\breve{F}_{k,p}^{(l)}H_{k,p'}^{(l')*}+\alpha\breve{F}_{k,p}^{(l)}=H_{k,p}^{(l)*}, l=1,...,NP, \tag{3.24}$$

where the correlation coefficient ρ is defined as in equation 3.18 and reproduced in equation 3.25 for a given user p and iteration i.

$$\rho_p^{(i)}=\frac{1}{2N}\sum_{n=0}^{N-1}\left(\left|\Re\left\{\bar{s}_{n,p}^{(i)}\right\}\right|+\left|\Im\left\{\bar{s}_{n,p}^{(i)}\right\}\right|\right). \tag{3.25}$$

So, the feedback coefficients are given by

$$B_{k,p}^{(p')}=\sum_{l=1}^{NP}F_{k,p}^{(l)}H_{k,p'}^{(l)}-\delta_{p,p'}, \tag{3.26}$$

with $\delta_{p,p'}=\begin{cases}1 & if \quad p\neq p'\\ 0 & if \quad p=p'\end{cases}$.

3.1.5 IB-DFE receiver performance

The IB-DFE receiver decodes the HeNB's L transmissions up to N_{iter} iterations. The estimated data symbol $\tilde{S}_{k,p}^{(i)}$, for a given iteration i and HeNB p is

$$\tilde{S}_{k,p}^{(i)}=F_{k,p}^{(i)^T}Y_k-B_{k,p}^{(i)^T}\bar{S}_k^{(i-1)} \tag{3.27}$$

where $F_{k,p}^{(i,l)^T}$ and $B_{k,p}^{(i,l)^T}$ with $l=1,2,...,L$ are the feedfoward and feedback coefficients respectively. $\bar{S}_{k,p}^{(i-1)}$ with $p=1,..,P$ are the soft decision estimates from the previous iteration for all HeNBs. $\bar{S}_{k,p}^{(i-1)}$ can be related to symbols hard decisions, $\hat{S}_{k,p}^{(i-1)}$ as

$$\bar{S}_{k,p}^{(i-1)}\simeq P^{(i-1)}\hat{S}_{k,p}^{(i-1)} \tag{3.28}$$

$$\hat{S}_{k,p}^{(i-1)}=P^{(i-1)}\Delta_k \tag{3.29}$$

where $P^{(i-1)}=diag(\rho_1^{(i-1)},...,\rho_P^{(i-1)})$ are the correlation coefficients and $\Delta_k=[\Delta_k^{(1)},...,\Delta_k^{(P)}]^T$ is a zero mean error vector. Assuming an QPSK constellation, the correlation coefficient

for a given HeNB p is

$$\rho^{(i-1)} = \frac{1}{2N} \sum_{n=0}^{N-1} \left| {\rho_{n,p}^{I}}^{(i-1)} \right| + \left| {\rho_{n,p}^{Q}}^{(i-1)} \right|. \tag{3.30}$$

For the first iteration ($i = 1$), $\bar{S}_{k,p}^{(i-1)}$ is a null vector and $P^{(i-1)}$ is a null matrix. As aforementioned, the $F_{k,p}^{(i,l)}$ and feedback $B_{k,p}^{(i)}$ coefficients are selected to minimize the SINR, for a given packet and a given iteration. This optimization problem can be written as the minimization of MMSE, $\mathbb{E}\left[\left|S_{k,p} - \tilde{S}_{k,p}^{(i)}\right|^2\right]$, of $S_{k,p}$:

$$\mathbb{E}\left[\left|\left({F_{k,p}^{(i)}}^T (H_k^T S_k + N_k)\right) - \left({B_{k,p}^{(i)}}^T P^{(i-1)}(P^{(i-1)} S_k + \Delta_k) + \Gamma_p S_k\right)\right|^2\right]. \tag{3.31}$$

To obtain the optimal coefficients,$F_{k,p}^{(i)}$ and $B_{k,p}^{(i)}$, under the MMSE criterion , the gradient of the Lagrange function is applied to equation 3.31:

$$\nabla J = \nabla\left(\mathbb{E}\left[\left|S_{k,p} - \tilde{S}_{k,p}^{(i)}\right|^2\right] + (\gamma_p^{(i)} - 1)\lambda_p^{(i)}\right) \tag{3.32}$$

conditioned to

$$\gamma_p^{(i)} - 1 = \frac{1}{N} \sum_{k=0}^{N-1} \sum_{l=1}^{L} F_{k,p}^{(i,l)} H_{k,p}^{(l)} - 1. \tag{3.33}$$

The following set of equations

$$\begin{cases} \nabla_{F_{k,p}^{(i)}} J = 0 \\ \nabla_{B_{k,p}^{(i)}} J = 0 \\ \nabla_{\lambda_p^{(i)}} J = 0 \end{cases} \tag{3.34}$$

were verified when

$$\gamma_p^{(i)} = 1. \tag{3.35}$$

For a single HeNB p transmitting data, i.e. without collisions, results

$$\gamma_p^{(i)} = 1, \tag{3.36}$$

$$B_{k,p}^{(i)} = \sum_{l=1}^{L} F_{k,p}^{(i,l)} H_{k,p}^{(l)} - \gamma_p^{(i)}, \tag{3.37}$$

$$F_{k,p}^{(i,l)} = \frac{\gamma_p^{(i)} H_{k,p}^{(l)*}}{\frac{\sigma_N^2}{\sigma_S^2} \sum_{l=1}^{L} \left| H_{k,p}^{(l)} \right|^2}. \tag{3.38}$$

$$\sigma_p^{2(i)} = \frac{1}{N^2} \sum_{k=0}^{N-1} \mathbb{E} \left[\left| \tilde{S}_{k,p}^{(i)} - S_{k,p} \right|^2 \right]. \tag{3.39}$$

Assuming the Gaussian behavior of the overall interference N_k that affects the symbol estimation, in accordance to [37], the symbol error probability P_s for a QPSK constellation is denoted by

$$P_s \simeq 2P_e \left(\eta_k > \sqrt{E_b} \right) = 2P_e \left(\frac{\eta_k}{\sigma_p} > \sqrt{\frac{E_b}{\sigma_p^2}} \right) = 2Q \left(\sqrt{\frac{E_b}{\sigma_p^2}} \right), \tag{3.40}$$

where $Q(x)$ is the well known Gaussian error function. Assuming that $E_b = 1$, the *Bit Error Rate* (BER) for a given HeNB p is

$$BER_p^{(i)} \simeq Q \left(\frac{1}{\sigma_p^{(i)}} \right). \tag{3.41}$$

For an uncoded system with independent and isolated errors, the PER for a fixed packet size of M bits is

$$PER_p^{(i)} \simeq 1 - \left(1 - BER_p^{(i)} \right)^M. \tag{3.42}$$

PER values are used to compute the HeNBs associated throughput at the receiver, denoted as

$$Th = \frac{W(1 - PER)}{L}, \tag{3.43}$$

where W represents the data bit rate and L denotes the number of packet transmissions used in the applied MPD technique (explained in section 3.1.4).

3.2 Femtocell interference characterization

This dissertation analyses the performance of the IB-DFE receiver when multiple femto BSs (HeNBs) transmit. A SC-FDE downlink channel is considered. For the receiver algorithm [37], using the receiver performance model presented in the subsection above can be used to characterize the system performance. The PER and BER are defined as a function, $< BER; PER >= f(H_k; Eb/N_0)$, which depends on the channel and on the transmission power. The energy per bit to noise power spectral density ratio, Eb/N_0, is an important parameter in digital communication or data transmission. It is a normalized SNR measure. Eb/N_0 is equal to the SNR divided by the link spectral efficiency in (bit/s)/Hz, where the bits in this context are the transmitted data bits. The SINR is normally used to characterize the interference caused by others transmissions in the reception at the UE of the desired signal. It is defined as

$$SINR = \frac{P_R}{P_{noise} + P_I} \tag{3.44}$$

where P_R and P_I denote the received power of the, desired signal from $HeNB_1$ and the signal from the P-1 interfering HeNBs. The received signal strength goes down as the *Pathloss* (PL) (explained in section 3.3) increases with the distance from the serving HeNB. The reception power is calculated using

$$P_T - PL, \tag{3.45}$$

where P_T denotes the HeNB transmit power and PL represents the path loss value associated to each link $HeNB - UE$.

3.3 Propagation Model

The receiver performance is strongly influenced by the characteristics of the channel. These characteristics depend upon the distance between the two antennas (transmitter and receiver) and the signal path(s). To support the development of 4G, ITU-R has adopted a number of models [38] to characterize different transmission scenarios, including: *Urban Macro-cell scenario* (UMa), *Urban Micro-cell scenario* (UMi) and Indoor Hotspot scenario(InH). For distances between 3 and 150 meters, common in femtocells hotspot, the InH was chosen. The propagation condition, LoS or NLoS, is assigned based on the physical distance (UE - HeNB) and the associated PL is computed as despited in equation 3.46, for each HeNB - UE communication link.

$$PL \begin{cases} LoS = 16.9 \times log_{10}(d) + 32.8 + 20 \times log_{10}(f_c) & if \quad d < 10 \\ NLoS = 43.3 \times log_{10}(d) + 11.5 + 20 \times log_{10}(f_c) & if \quad d \geq 10 \end{cases}, \tag{3.46}$$

where d represents the distance between the p^{th} HeNB and the UE given in m and f_c denotes the HeNB carrier frequency given in GHz. The effect of both pathloss models adopted in terms of E_b/N_0(dB)$= P_T - PL - P_{noise}$, is depicted in figure(3.8). NLoS and LoS are valid between 3 and 100 m and 10 and 150 m respectively, where E_b/N_0 from LoS is higher than from NLoS channels, for distances above 18 m.

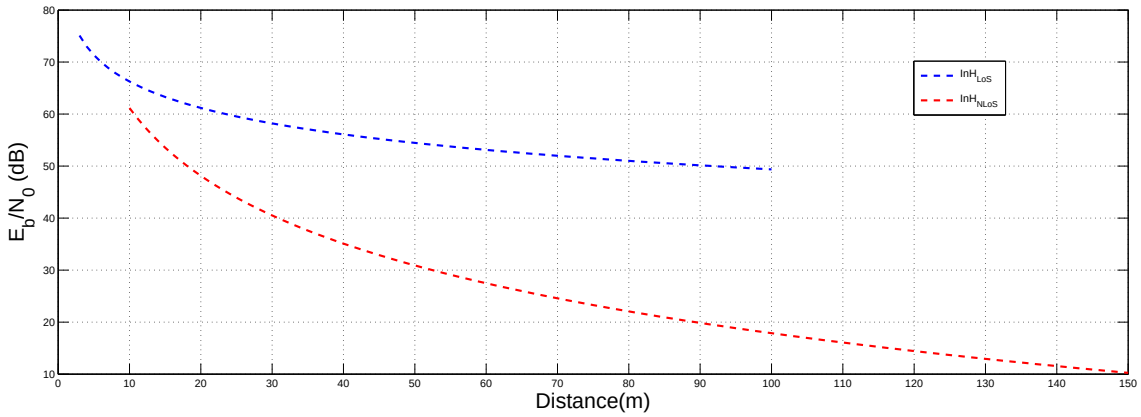

Figure 3.8: Propagation Models InH: LoS and NLoS E_b/N_0 influence

3.4 Channel coefficients generation

In general, the received signal can be obtained by convolving (in TD) or multiplying (in FD) the transmitted signal with the impulse response of the channel. Therefore, the received signal is:

$$Y_k = H_k S_k + N_k, \tag{3.47}$$

where H_k and N_k are the FD channel response and the noise respectively. The H_k coefficient for a transmitter and a receiver is defined by a set of signal paths or rays, each with a distinct delay and attenuation, characterized by the tap delay or clustered delay line model :

$$\begin{bmatrix} P_{(1)} & \tau_{(1)} \\ \vdots & \vdots \\ P_{(C)} & \tau_{(C)} \end{bmatrix} \tag{3.48}$$

where C denotes the considered number of clusters. A cluster is characterized as a propagation path diffused in space, either or both in delay and angle domains [38] or simply as a set of rays. Each cluster delay and power, represented by $\tau_{(c)}$ and $P_{(c)}$ respectively, are computed as follows.

3.4.1 Cluster delay generation

Depending if the propagation condition assigned was LoS or NLoS, the set of delays $\tau_{(c)}$ are generated using a uniform distribution as followed, where r_τ is the delay distribution proportionality factor, σ_τ is the delay spread and $X_c \sim Uni(0,1)$.

$$\tau_c^{'} = -r_\tau \sigma_\tau ln(X_c) \tag{3.49}$$

Then the delays are normalized (by subtracting the minimum delay) and sorted in descending order.

$$\tau_c = sort(\tau_c^{'} - min(\tau_c^{'})) \tag{3.50}$$

In the case of a LoS path, an additional scaling was done to compensate peak addition to delay spread,

$$\tau_c^{LoS} = \frac{\tau_c}{D}, \tag{3.51}$$

where D is the Ricean K-factor dependent, scaling constant given by:

$$D = 0.7705 - 0.0433K + 0.0002K^2 + 0.000017K^3 \tag{3.52}$$

3.4.2 Cluster power generation

Each cluster power or attenuation, $P'_{(c)}$ is computed based on the above explained delay generation. $P'_{(c)}$ has an exponential distribution [38],

$$P'_{(c)} = exp(-\tau_c \frac{r_\tau - 1}{r_\tau \sigma_\tau}).10^{\frac{-Z_{(c)}}{10}}, \tag{3.53}$$

where $Z_{(c)} \sim N(0, \zeta^2)$ denotes the shadowing term.
Then $P'_{(c)}$ is normalized,

$$P_c = \frac{P'_c}{\sum_{c=1}^{C} P'_c}, \tag{3.54}$$

and in the case of LoS path, an additional specular component is added to the first cluster

$$P_{1,LoS} = \frac{K_R}{K_R + 1}, \tag{3.55}$$

so the LoS cluster powers are

$$P_{c,LoS} = \frac{1}{K_R + 1} \frac{P'_c}{\sum_{c=1}^{C} P'_c} + \delta(c-1) P_{1,LoS}, \tag{3.56}$$

In this performance model it is assumed that the $HeNB_1$ transmits during L slots and that the other $P-1$ also transmit simultaneously during the L slots. Let $\{s_{n,1}; n = 0, 1, ..., N-1\}$ denote the data block from the $HeNB_1$ and $\{s_{n,p}; n = 0, 1, ..., N-1\}$ from the $HeNB_p$ and their corresponding frequency domain blocks, after applied an size-N DFT operation, $\{S_{k,1}; k = 0, 1, ..., N-1\}$ and $\{S_{k,p}; k = 0, 1, ..., N-1\}$, respectively, where N denotes the

number of data symbols.

The received content at the *UE*, $\{Y_k; k = 0, 1, ..., N-1\}$, depends on the L channel realizations of the P HeNBs ($H_{k,p}; p = 1, ..., P$), P HeNBs transmitted signals ($S_{k,p}; p = 1, ..., P$) and associated channel's noise (N_k), and is given by equations 3.19 and 3.20 reproduced bellow by convenience.

$$Y_k^{(l)} = H_{k,1}^{(l)} S_{k,1} + \cdots + H_{k,P}^{(l)} S_{k,P} + N_k^{(l)}, \tag{3.57}$$

or the expanded expression

$$\begin{bmatrix} Y_k^{(1)} \\ \vdots \\ Y_k^{(L)} \end{bmatrix} = \begin{bmatrix} H_{k,1}^{(1)} & \cdots & H_{k,P}^{(1)} \\ \vdots & \ddots & \vdots \\ H_{k,1}^{(L)} & \cdots & H_{k,P}^{(L)} \end{bmatrix} \begin{bmatrix} S_{k,1} \\ \vdots \\ S_{k,P} \end{bmatrix} + \begin{bmatrix} N_k^{(1)} \\ \vdots \\ N_k^{(L)} \end{bmatrix}, \tag{3.58}$$

where H_k denotes the channel frequency response computed from tap delay values (3.48) and N_k denotes the corresponding channel noise.

3.4.3 Channel modeling

The channel model is influenced by the interference pattern, modeled by ITU-R [38], and by the spatial distribution of the HeNBs and the UEs. The two contributions are modeled in the $H_{k,l}$ matrix coefficients. The signal attenuation associated to the transmission from a HeNB and the UE is defined by the PL, which depends of the distance and the channel model and can be calculated using [38] (see equation 3.46),

$$\xi(l, p) = 10^{\frac{-PL(p)}{20}}. \tag{3.59}$$

The coefficients that form the H matrix are calculated assuming a reference transmission power, so the equivalent PL is defined as $P_L = P_{T_{ref}} - P_R$, where $P_T = P_R + PL$. Finally, the coefficients for the L channel realizations of the p^{th} HeNB are given by

$$\xi(l, p) H_{k,p}^{(l)}. \tag{3.60}$$

So the received content at the UE, given by equation 3.57, can be rewritten as

$$Y_k^{(l)} = \xi(l,1)H_{k,1}^{(l)}S_{k,1} + \sum_{p=1}^{P-1}\xi(l,p)H_{k,p}^{(l)}S_{k,p} + N_k^{(l)}, \tag{3.61}$$

for a scenario with P-1 interfering HeNBs.

The PER values for the iterative receiver can be calculated extending the models introduced in sections 3.1.3 and 3.1.4. The linear one is a special case of the IB-DFE, where the number of iterations (N_{iter}) is equal to 1.

3.5 Performance results

This section presents a set of performance results for the proposed IB-DFE receiver in time-varying channels. It was considered a SC-FDE modulation, with FFT-block of N=256 data symbols and a CP of 32 symbols, longer than overall delay spread of the channel. The simulations were performed in MATLAB® following ITU-R M.2135 simulation guideline using the key simulation parameters summarized in Table 3.1.

HeNB transmit power	21 dBm
Bandwidth	20 MHz
Minimum distance (d) between UE serving HeNB	3 m
Carrier frequency (f_c)	3.6 GHz
Thermal noise level	-174 dBm/Hz
Channel model/PL	ITU-R M.2135 InH : LoS or $NLoS$

Table 3.1: Simulation parameters

For each value of D (distance between serving HeNBs) the UE reception performance was measured considering the coverage range of $HeNB_1$ and a granularity of one meter, for each value of D considered. The distance between HeNBs (D) was set between 5 and a maximum value defined by the propagation model adopted upper limit [38], considering increments of 5 meters. The performance results are presented to a maximum distance of:

$D = 100$ without retransmissions and $D = 200/250$ (for P=3/P=2)$D = 200$, to evaluate the retransmission's potential gains. To evaluate the receiver performance three main study scenarios were defined(explained and discussed in detailed in the follow subsections):

1. without interference - 1 HeNB; 1 UE (see section 3.5.1)

2. with simple interference - 2 HeNBs; 1 UE (see section 3.5.2)

3. with complex interference - 3 HeNBs; 1 UE (see section 3.5.3)

It is important to refer that the number of uncorrelated channels is a receiver algorithm [37] input variable, chosen according to the desired precision level.

3.5.1 Without interference

The experiment performed is illustrated in figure 3.9. One HeNB transmits to a UE.

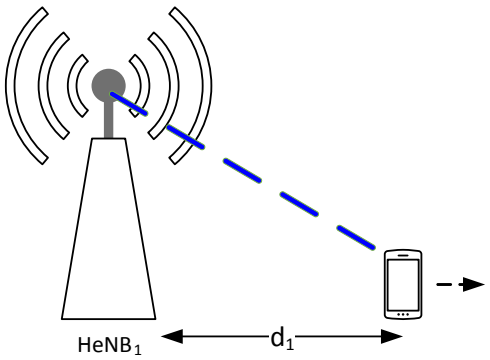

Figure 3.9: Simulation scenario used to find $HeNB_1$ range, with P=1 and L=1

The average range of the $HeNB_1$ transmission without interferences (i.e. with a single HeNB) was measured in these set of simulations. The result is despited in figures 3.10 and 3.11, which show that to have a PER below 1% the *UE* should be up to 75 meters far from the $HeNB_1$ or in terms of SNR, it should not be bellow 15 dB.

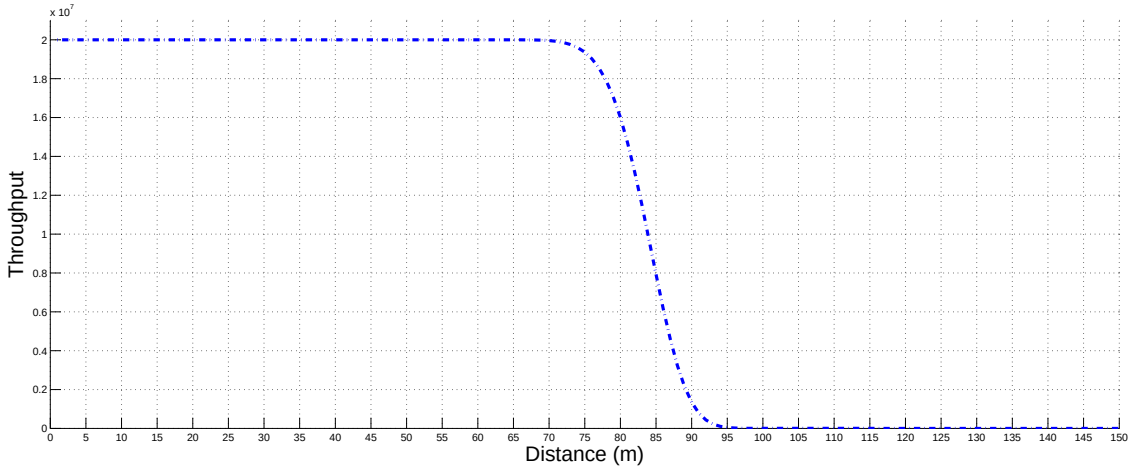

Figure 3.10: Throughput as a function of distance $HeNB_1$ - UE

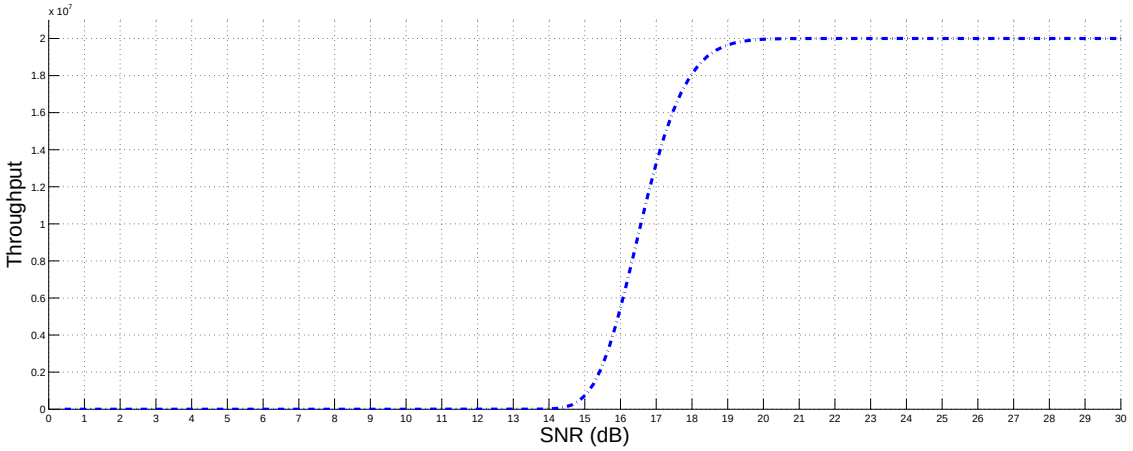

Figure 3.11: Throughput as a function of SNR

3.5.2 Simple interference

The experiment performed is illustrated in figure 3.12. One HeNB transmits to a UE that receives interference from another HeNB.

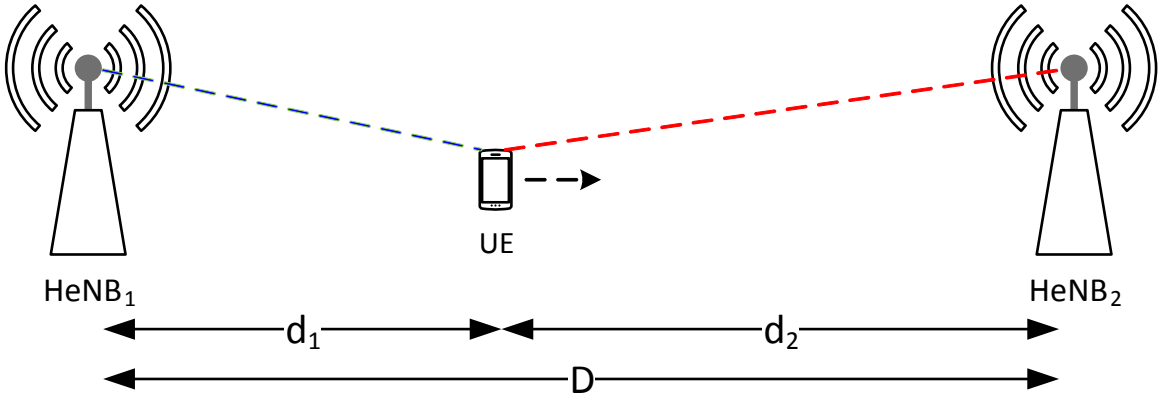

Figure 3.12: Simple interference simulation scenario used to evaluate receiver performance, with P=2 and L=1

Two kinds of receivers were analyzed: linear receivers and IB-DFE receivers considering 4 iterations ($N_{iter} = 4$). The simulation performed with 2 HeNBs simultaneously transmitting to an UE, in which was applied an linear FDE receiver is depicted in figures 3.13 and 3.14.

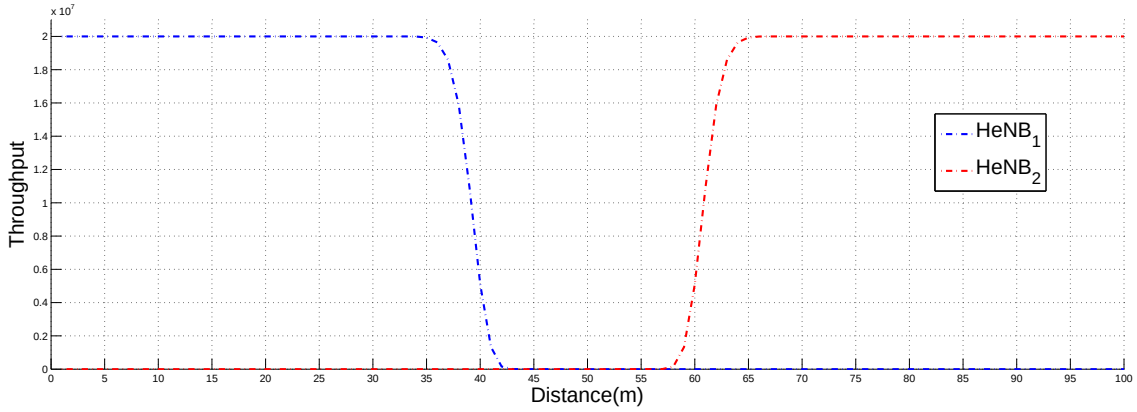

Figure 3.13: Throughput as a function of distance $HeNB_1$ - UE and $HeNB_2$ - UE

It is observable a significant $HeNB_1$ coverage range decrease, due to the interference from $HeNB_2$. 10 dB is the minimum SINR value that allows experiencing the maximum throughput. The transition between the LoS and the NLoS model is noticeable for the distances of 10 and 90 meters.

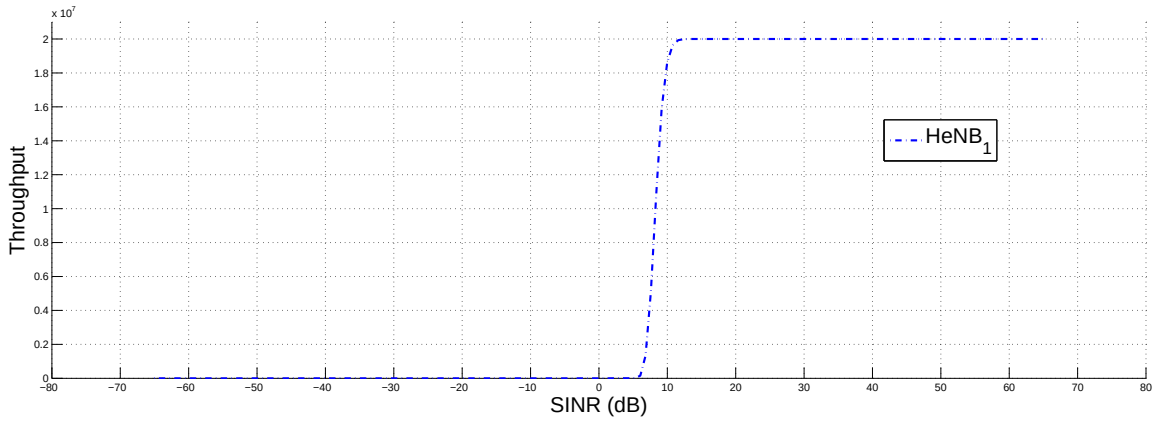

Figure 3.14: Throughput as a function of SINR

In figure 3.15 is shown the results when the iterative receiver is used. It can be seen that IB-DFE increases the coverage range of the HeNB because IB-DFE SIC technique is capable of recovering the received signal within the coverage range as long as the received power from both HeNBs differ at least 5 dB as shown in figure 3.16.

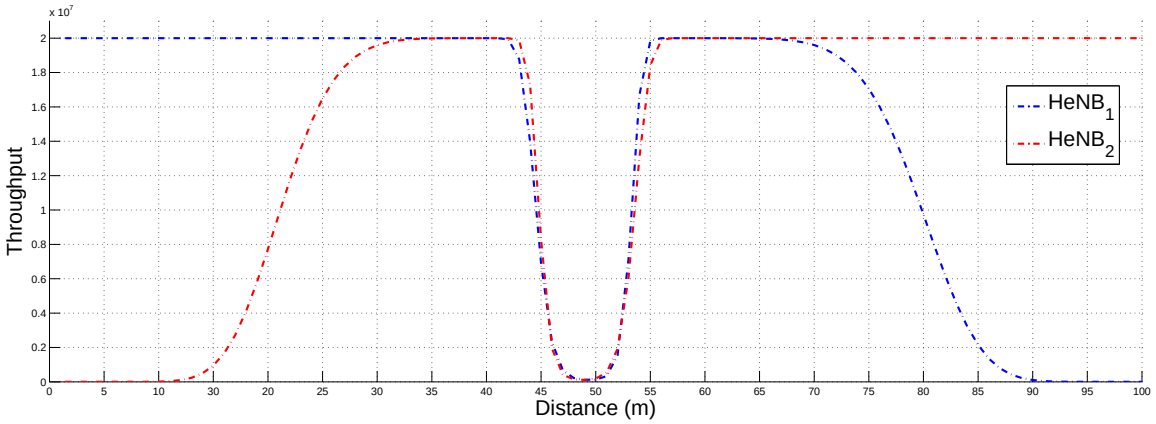

Figure 3.15: Throughput as a function of distance $HeNB_1$ - UE

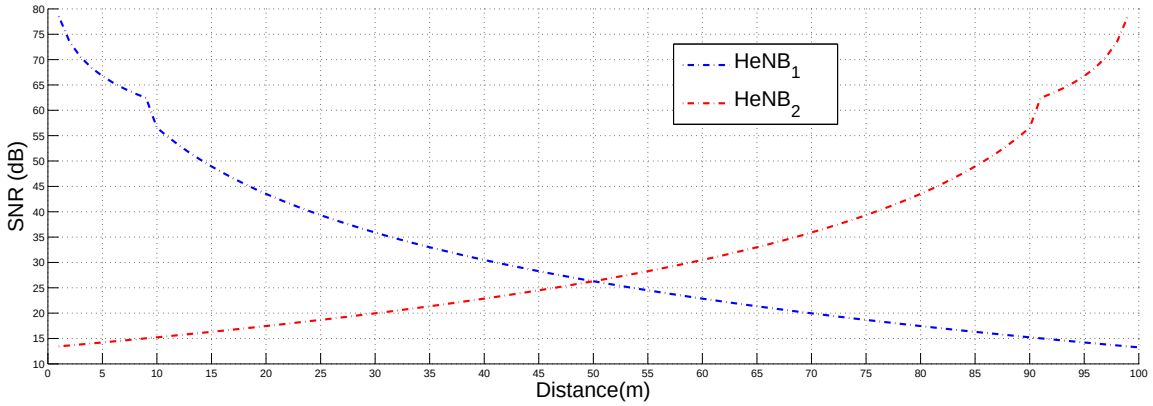

Figure 3.16: $HeNB_1$ and $HeNB_2$ SNR as function of distance

When the two reception powers are similar, IB-DFE fails, and a dead zone exists in the coverage area. In order to improve the coverage range and eliminate that dead zone, multiple copies of the packets can be transmitted. The next experiment in figure 3.17 depicts the result of applying the MPD technique, where it is required one retransmission per HeNB involved in the collision, so L=2.

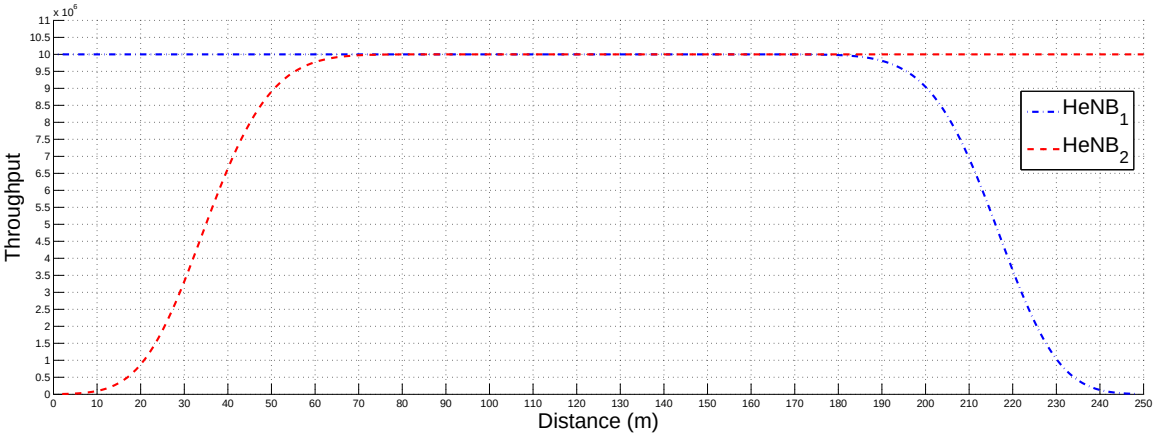

Figure 3.17: Throughput as a function of distance $HeNB_1$ - UE

It is clear that the MPD technique appliance not only resolved the coverage hole or dead zone problem, as well as significant enhanced the $HeNB_1$ coverage area. However, as shown in equation 3.43 it also reduce the available bandwidth.

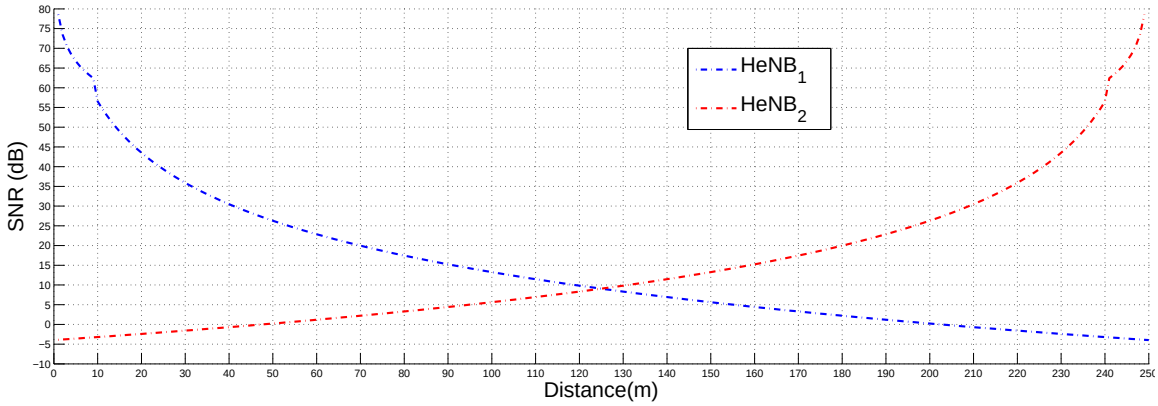

Figure 3.18: $HeNB_1$ and $HeNB_2$ SNR as function of distance, with L=2

3.5.3 Complex interference

The experiment performed is illustrated in figure 3.19. One HeNB transmits to a UE that receives interference from two HeNBs.

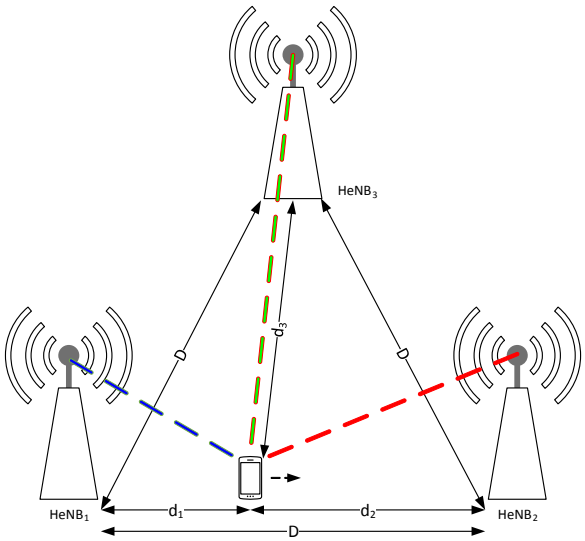

Figure 3.19

As previously depicted in the simple interference scenario 3.5.2, the IB-DFE SIC technique is capable of recovering the received signal under a minimum difference in the received powers from all HeNBs difference; The capacity to recover from collisions remains with three concurrent HeNBs, although it presents a larger dead zone in the coverage area, meaning that it needs a greater difference in the received power from all HeNBs.

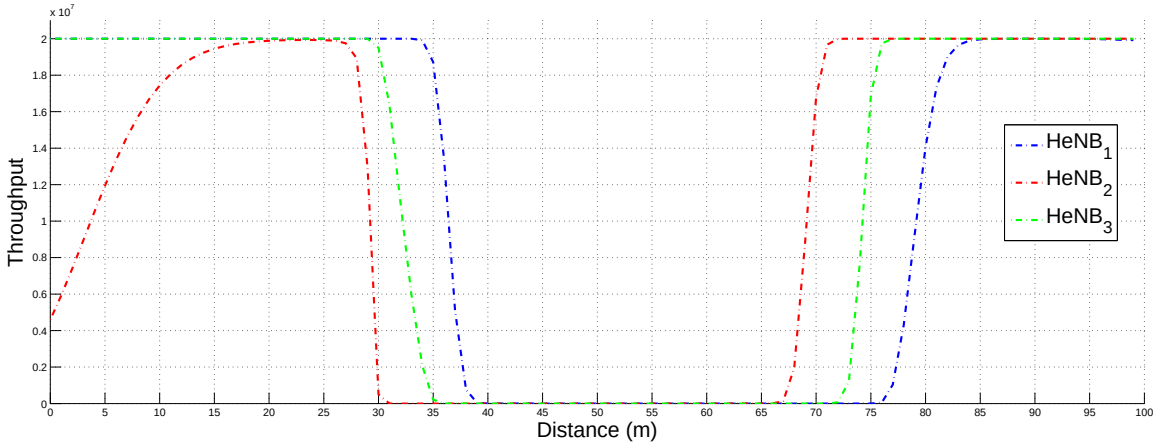

Figure 3.20: Throughput as a function of distance $HeNB_1$ - UE, $HeNB_2$ - UE and $HeNB_3$ - UE

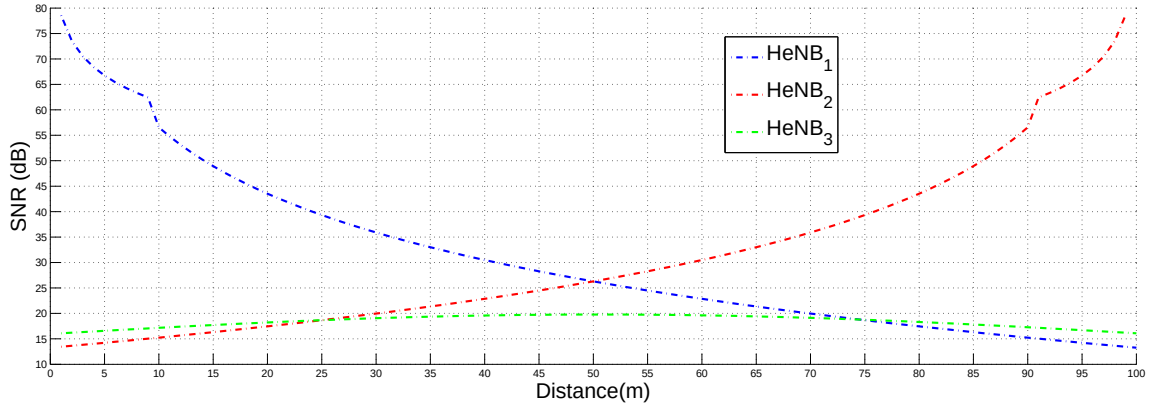

Figure 3.21: $HeNB_1$, $HeNB_2$ and $HeNB_3$ SNR as function of distance

When the MPR technique is applied, i.e. when packets are transmitted twice per HeNB involved in the collision, it is observable a coverage gain as expected, although less significant than the one verified in the simple interference scenario.

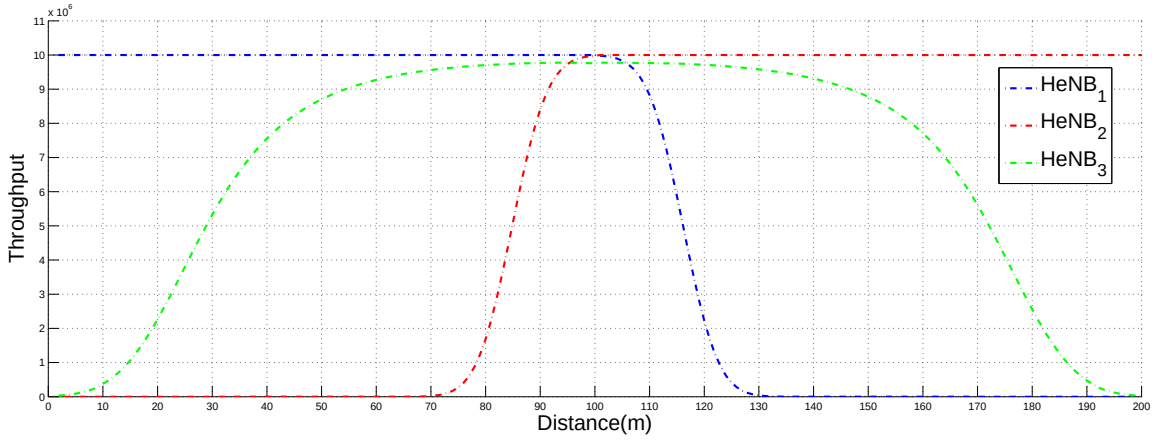

Figure 3.22: Throughput as a function of distance $HeNB_1$ - UE, $HeNB_2$ - UE and $HeNB_3$ - UE

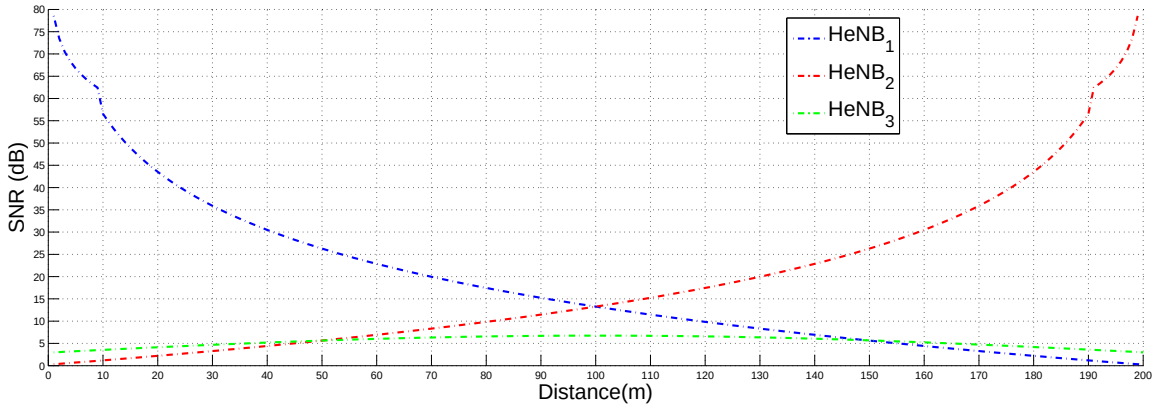

Figure 3.23: $HeNB_1$, $HeNB_2$ and $HeNB_3$ SNR as function of distance, with L=2

As depicted in figures 3.22 and 3.23, high values of throughput can be achieved with low values of SNR when the MPR technique is applied to resolve the three collisions. Due to the serial nature of the receiver considered, with 4 iterations, it can resolve collisions of up to 4 UEs, failing for the 5th less powerful UE signal. It is also important to refer that for $\dot{=}10m$ there is a small variance in the SNR value , owing to the change of propagation conditions, i.e. PL models (LoS to NLoS)(see section 3.3).

Chapter 4

Green concern

The energy consumption is viewed as one of the near-future major concerns due to the rapid growth of cellular networks, typically performance-oriented planned. Moreover the exponential growth of mobile data traffic [39], requiring higher network capacity equally leads to an increase of the energy consumption. These are the main reasons why great attention is currently devoted to this problematic [40]. In this chapter, a brief introduction to Green Communication(GC) is carried out. This introduction includes the main concerns and proposed technologies. Lastly, it is explained and tested the green algorithm proposed in this thesis.

4.1 Green Communications

The rising energy costs and carbon footprint of operating cellular networks have led to an emerging trend of addressing energy-efficiency amongst the network operators and regulatory bodies [41], [42]. From an operator's perspective, reducing energy consumption will also translate to lower *Operational expenditure* (OPEX) costs. Telecommunication networks and broadband access are proved to consume a huge amount of energy for data delivery and this consumption is mainly drawn from BSs and the increasing number of deployed BSs to address high capacity networks. In order to achieve a favorable tradeoff between energy consumption and performance, an efficient use of the available resources (BSs) should be done. This is the main idea behind the recently emerged concept of GC. Following this GC notion, several schemes and technologies were proposed. Taking

advantage of the network traffic load fluctuation phenomenon, both academic and industry studies proposed some switching on/off schemes [40]. Another popular approach is to adjust BS's transmit power, which leads to variable cell sizes, i.e. different coverage areas per BSs. This approach is commonly known as Cell-Zooming [43]. Finally, taking advantage of the emerged low power BSs, namely femtocells, some multi-cell cooperation approaches were proposed [40]. The femtocells deployment is seen as the most promising solution to enhance mobile networks capacity and coverage, and also constitutes a huge step to achieve this green concern [44]. Although being more energetic efficient compared to eNBs, the HeNBs low power nature and consequently low coverage area, leads to a network densification, i.e. the deployment of a large number of HeNBs per area, raising questions about the corresponding electrical energy consumption footprint. The main proposal of this section is to improve of HeNBs power amplifiers, using IB-DFE transmission scheme in the DL and to reduce the number of active HeNBs, applying an switching-off algorithm according to traffic load demands. The final goal is to achieve the main purpose of green communications, energy saving in BSs.

4.2 Green algorithm

Given the global increasing concerns (specially from the telecommunications community) about the energetic consumption, it is proposed an UE - HeNB association algorithm, whose main goal is to reduce the total BS energy consumption, adapting the network layout according to data traffic demands, i.e. reducing the number of HeNBs required to serve UEs in their deployment area.

4.2.1 System characterization

The DL of a HNet with a dedicated channel deployment of macro and femto BSs is considered for this study, assuming the SC-FDE as transmission scheme. All UEs are under the eNB coverage. The macro-cell is seen as a fall-back solution applied when there are no available HeNBs or when the femtocell network layer reaches its maximum capacity. An UE never experiences lack of coverage.

The proposed algorithm iteratively combines a switch-off scheme (turns off BSs) with

the previous explained and tested IB-DFE receiver (see chapter 3), in order to achieve a favorable tradeoff between EE and QoS in the femtocell layer of the simulated wireless network. To calculate the PL gains between HeNBs and UEs an indoor hotspot channel model(InH) was used, based on ITU-R M.2135-1 indoor test environment [38], previously explained in section 3.3. For simplicity, it was assumed that the deployed HeNBs were configured to work in OA mode (see section 2.2.3), thus avoiding the UE association security issues/constraints.

As this algorithm intends to reduce the energy consumption without compromising the network performance, it was defined that a HeNB serves an UE only if it can guarantee a minimum level of QoS. It is assumed that the total load of a HeNB, ρ, should be below 90% when more than one UE is associated. So for each $UE_{(i)}$ the set of HeNBs that can serve it without violating the following capacity constraints, ψ, is found:

$$\begin{cases} \rho_{(j)} \leq 0.9 & if \quad N > 1 \\ \rho_{(j)} \leq 1 & if \quad N = 1 \end{cases}, \tag{4.1}$$

where N denotes the number of UEs associated to a HeNB and ρ denotes the HeNB total traffic load given by

$$\rho_{(j)} = \sum \lambda_{eff(i,j)}. \tag{4.2}$$

$\lambda_{eff(i,j)}$ denotes each UE portion in the HeNB traffic load, including retransmissions due to error recovery. An upper bound can be defined assuming that errors are always recovered. Therefore, λ_{eff} can be computed based on:

$$\lambda_{eff(i,j)} = L_{(i)} \times \frac{\lambda_{(i)}}{1 - PER_{(i,j)}}, \tag{4.3}$$

where $L_{(i)}$ and $PER_{(i,j)}$ represent the number of concurrent transmissions (see MPD explanation in 3.1.4) and the average packet error rate, per HeNB for UE, respectively, whereas $\lambda_{(i)}$ denotes i^{th} UE traffic load requirement. All HeNBs included in an UE-HeNB association that respect the capacity constraints shown in equation 4.1 are added to a group, named ψ.

It is from this set of possible associations, that, according to the follow explained conditions, it is chosen the HeNB to provide coverage to the UE. The five conditions defined, are showed bellow ordered by deceasing precedence:

1. Highest ratio, $\frac{\rho_{(j)}}{\lambda_{eff(i,j)}}$.

2. Minimum distance to UE ($d_{i,j}$).

3. Highest ρ.

4. Lower λ_{eff}.

5. More attached UEs.

Based on [20], it was assumed that the power consumption of a HeNB under maximum load is 15 Watts, which is divided in two portions: 2/3 associated to power dependency and 1/3 to power offset consumption (independent of HeNB transmit power (P_T)). It was fixed that all HeNBs have the same transmit power (P_T) and load requirement λ. Therefore, the power consumption of a HeNB with traffic load ρ is:

$$P_{f(j)}(\rho) = 10 \times (\rho + \alpha \times (1 - \rho)) + 5 \times \beta, \tag{4.4}$$

where $\alpha, \beta \in [0$ (offsets $= 0), 1$ (load independent)] represent the *HeNB* energy profile factor [20]. Finally, HeNBs may work in one of two distinct modes:

- Active mode - The HeNB is serving his associated *UE*s holding a certain ρ value, subsequently, the power consumption P_f is given by equation 4.4.

- Sleeping mode - The HeNB is turned off, meaning the power consumption $P_f = 0$.

4.2.2 Algorithm

The procedure of the algorithm is described as follows. The algorithm is presented bellow, identifying the most relevant Steps. Then each identified step is explained.

```
for each λ do
    repeat
        for each UE do
            for each HeNB do
                if active then
                    Compute distance to UE (Step 1);
                    if reachable then
                        Compute :
                        - PL (Step 2);
                        - PER (Step 3);
                        - λ_eff and ρ (Step 4);
                        if Respect capacity constraints then
                            Apply selection conditions on ψ(Step 5);
                        end
                        Associate to HeNB;
                    else
                        Associate to eNB
                    end
                end
            end
        end
        for All HeNBs do
            if presents ρ = 0 & All UEs served then
                Sleep Mode (Step 6);
            else
                Active Mode;
            end
        end
    until no possible changes in network layout;
    Compute total BSs energy consumption. (Step 7)
end
```

Step 1: For each UE $\{UE_{(i)}; i = 1, ..., I\}$ it is calculated the distance, $d_{i,j}$, to all reachable and active HeNB $\{HeNB_{(j)}; j = 1, ..., J\}$, where I and J represent the total number of UEs and $HeNB$s, respectively.

Step 2: The suitable PL model (LoS or NLoS), chosen from 3.46 is applied to each $d_{i,j}$ value, and the respective channel coefficients are computed (see section 3.4).

Step 3: For each UE, is applied the IB-DFE receiver function (with Niter=4)(see chapter 3) in order to compute the packet error rate $PER_{(i,j)}$ associated to each received signal from reachable HeNBs .

Step 4: The effective load λ_{eff} is computed using equation 4.3 and the capacity constraints 4.1 are applied, in order to select the set of available HeNBs (ψ).

Step 5: Each $UE_{(i)}$ selects among all HeNBs in set ψ, according to the conditions defined in section 4.2.1.

Step 6: All HeNBs with traffic load $\rho_{(j)} = 0$ when all reachable UEs are served (by another HeNB or by the eNB), are turned off i.e. they work in sleep mode in the following serving time.

Step 7: Finally it is computed the energy consumption 4.4, derived from the final network layout.

The algorithm ends when there are no changes from the previous iteration network layout, i.e. no changes in the total number of active HeNBs. The algorithm flowchart is presented bellow.

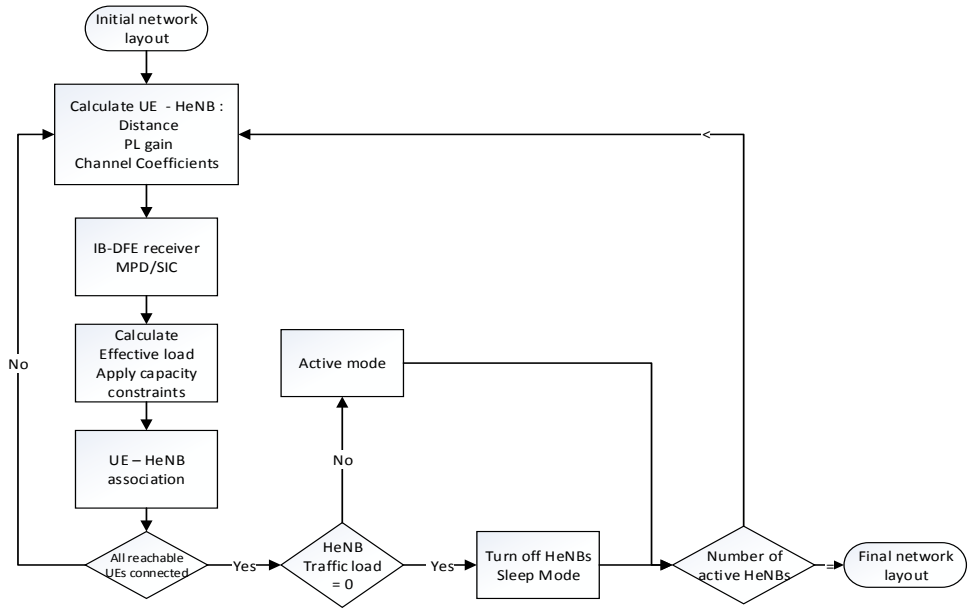

Figure 4.1: Green algorithm procedure

4.3 Simulation

The main purpose of this simulations is to investigate, in terms of energy efficiency, the influence of combining the use of an IB-DFE receiver and the switch-off BSs approach in a femtocells network. In order to validate the proposed algorithm a two tier network scenario, as depicted in figure 4.2, was chosen considering a HeNB dedicated channel deployment therefore, avoiding the cross-tier interference problems. Mobility was not considered.

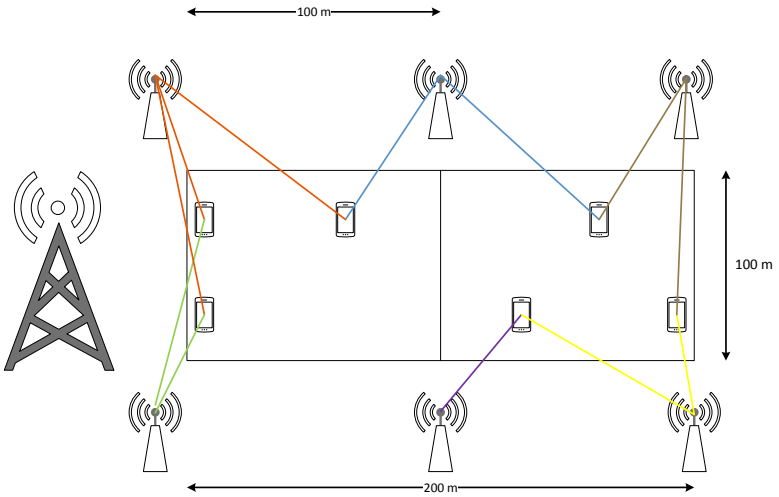

Figure 4.2: Simulation scenario

The algorithm applies MPR and cell zooming techniques, such as MPD and SIC, and Zoom in to zero (turning off the HeNBs) respectively. In order to evaluate the potential gains of the proposed algorithm, the simulations were performed in MATLAB® following ITU-R M.2135 simulation guideline using the key simulation parameters summarized in Table 4.1. Each UE is deployed under the coverage of two HeNB, to observe the influence of the applied techniques. The proposed algorithm changes the network layout according to mobile users load requirements λ. It was not considered heterogeneous traffic, i.e. is used the same λ for all UEs.

Central frequency (f_c)	3.4 GHz
HeNB transmit power (P_T)	-9 dB
Number of *HeNB*s	6
Number of *UE*s	6
Coverage (radius)	80 m
Deployment area	200 m × 100 m
Scheduling strategy	equal bandwidth per *UE*
Bandwidth	20 MHz
Thermal noise density	-174 dBm/Hz
Channel and path loss models	ITU-R M.2135-1
Load per UE (step value)	0.05 to 1 (0.05)

Table 4.1: Simulation parameters

4.3.1 Performance results

In this section, the simulation results are presented and discussed, regarding the appliance of the previously explained green algorithm (see section 4.2).

Figure 4.3 depicts the number of active HeNBs based on the load requirement per UE, considered uniform. It is notable that it is only necessary 50% of the HeNBs in the active mode, for λ values under 0.5 , to achieve the desired performance and consequent QoS level.

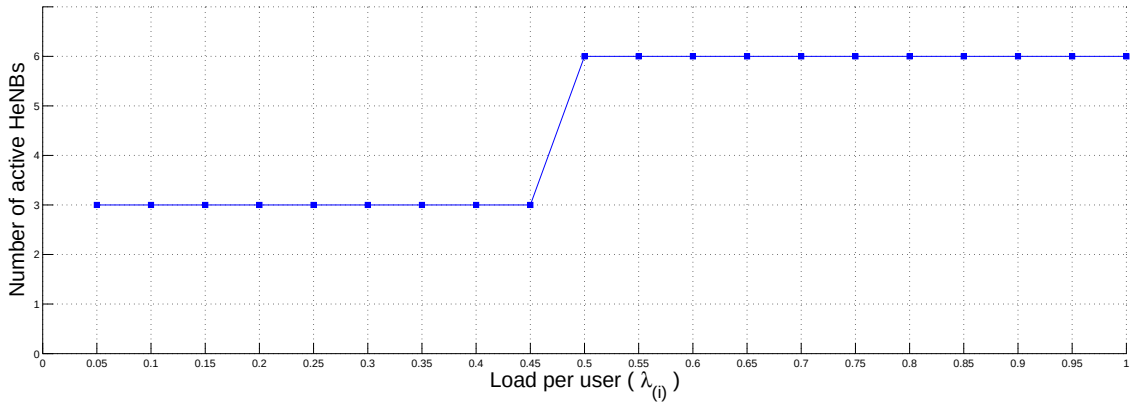

Figure 4.3: Number of active HeNBs as a function of UE load requirement, λ

The reduction in the number of active base station is due to the association of multiple UEs to neighbor HeNBs, instead of using only one UE per HeNB. This joint association is visible in terms of energy consumption per HeNB represented in figure 4.4, and in terms of the total traffic load per HeNB, depicted in figure 4.5.

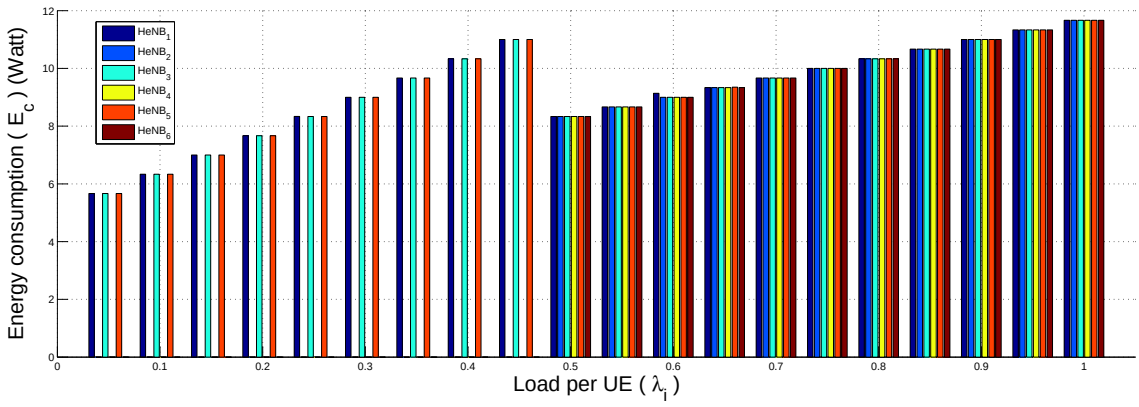

Figure 4.4: HeNBs energy consumption as a function of UE load requirement, λ

It is important to notice that for λ values under 0.5, the active HeNBs present higher energy consumption due to the higher traffic load associated to each one of them.

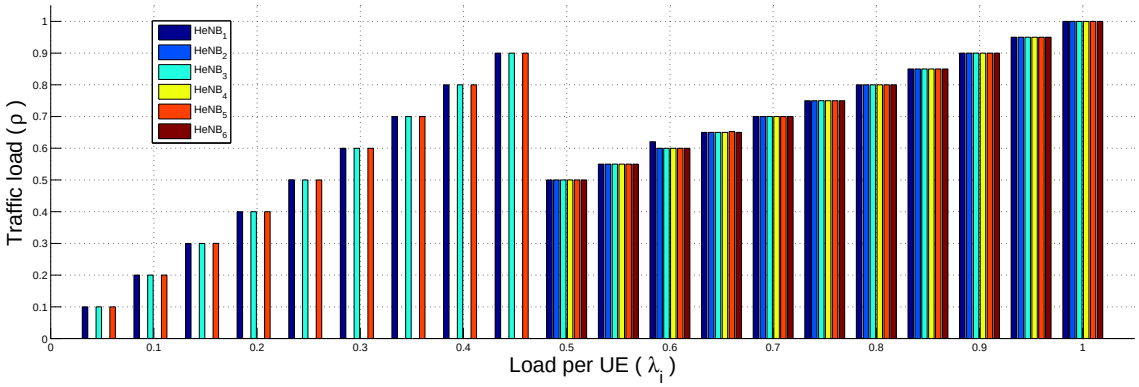

Figure 4.5: HeNBs total load ρ as a function of UE load requirement, λ

In consequence of this reduction in the number of active HeNBs, it is achieved a considerable energetic gain, specially for lower values of λ, as shown in figure 4.6.

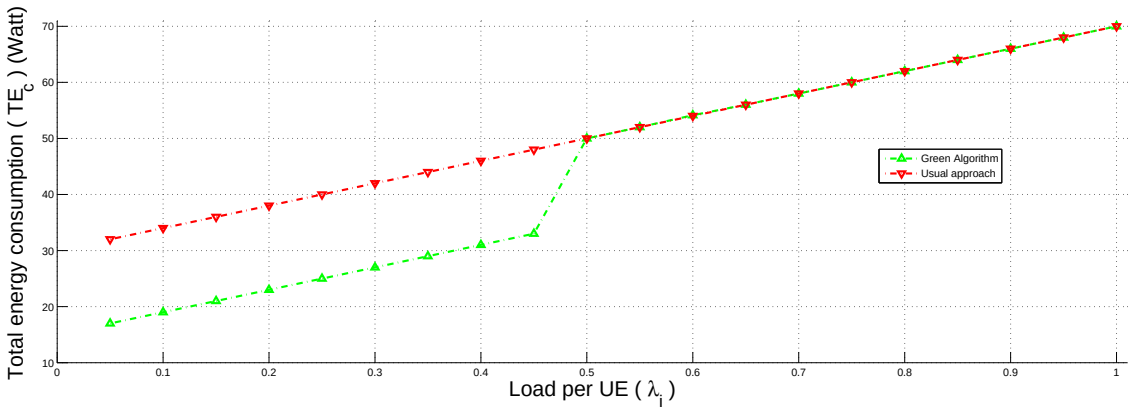

Figure 4.6: Total BS's energy consumption as a function of UE load requirement, λ

As there are only two concurrent HeNBs, the maximum number of retransmissions was limited to L=2, to avoid an excessive reduction in terms of available bandwidth. Owing to capacity constraints applied to guarantee a minimum level of QoS, for λ above 0.5 there is no visible energy gains since each HeNB can only have one UE associated to it, meaning that to ensure the total coverage all HeNBs have to be in active mode. In this simulation scenario there was no need to use eNB coverage, since the applied receiver resolves all interference problems and the same number of UEs and HeNBs were deployed.

Chapter 5

Conclusions

5.1 Final Considerations

This work intended to demonstrate the performance achievable of the MPR technique using an IB-DFE receiver in the DL of a LTE-A femtocell based network. As expected, it is shown in chapter 3 that the iterative SIC receiver presents pleasant performance results, enhancing the HeNB coverage range even in high interference scenarios. This receiver "only" recover the signal, it does not prevent the existence of dead zones. The MPR appliance revel to be very efficient in this undesirable coverage holes elimination. Although the applied MPR approach reduces the available bandwidth due to require multiple packet retransmissions. The IB-DFE receiver employing SIC was tested with up to three HeNBs, i.e. three possible collisions, but uses four iterations it is capable to efficiently resolve up to four collisions (see explanation of IB-DFE SIC receiver in section 3.1.4). The second part of this thesis (chapter 4) intended to prove the applicability of the receiver and techniques studied in chapter 3 to a simulated "real world scenario". Following the actual energy consumption increasing concerns, the receiver is used in a developed green association algorithm which employs an switch-off algorithm. The energy savings regarding the use of this algorithm shown in section 4.3.1 meet the main idea behind the recently emerged concept of GC (see section 4.1). Considerable energetic gains were achieved specially for lower load requirements. For higher load requirements it was not possible to turn off serving HeNBs due to capacity constraints applied to preserve the provided QoS. The overall results show that the employed and developed technologies

are a practicable solution to achieve a favorable trade-off between performance and EE in wideband wireless networks, answering to the global demands (high data rates) and concerns (low energy consumption and carbon footprint reduction).

5.2 Future Work

In this thesis it was employed SC-FDE in the LTE-A femtocell network DL, studying the performance of the MPR approach using an IB-DFE SIC receiver. Based on the pleasant performance results obtained in this thesis, it would be interesting to evaluate the performance of this iterative receiver and techniques(MPD and SIC) for both UL and DL communication side, combining them with other techniques such as:

1. Cooperation between BSs (CoMP) (see [45], [46])

2. Adjusting the BS transmit power(Cell zooming) (see [47], [48])

Bibliography

[1] V. Chandrasekhar, J. Andrews, and A. Gatherer, "Femtocell networks: a survey," *Communications Magazine, IEEE*, vol. 46, no. 9, pp. 59–67, 2008.

[2] J. Parikh and A. Basu, "LTE Advanced: The 4G mobile broadband technology," *spectrum*, vol. 5, no. 2.5, p. 30, 2011.

[3] D. Bai, C. Park, J. Lee, H. Nguyen, J. Singh, A. Gupta, Z. Pi, T. Kim, C. Lim, M.-G. Kim, *et al.*, "LTE-Advanced modem design: challenges and perspectives," *Communications Magazine, IEEE*, vol. 50, no. 2, pp. 178–186, 2012.

[4] A. Damnjanovic, J. Montojo, Y. Wei, T. Ji, T. Luo, M. Vajapeyam, T. Yoo, O. Song, and D. Malladi, "A survey on 3GPP heterogeneous networks," *Wireless Communications, IEEE*, vol. 18, no. 3, pp. 10–21, 2011.

[5] E. Dahlman, S. Parkvall, and J. Skold, *4G: LTE/LTE-Advanced for Mobile Broadband*. Academic Press.

[6] P. Bhat, S. Nagata, L. Campoy, I. Berberana, T. Derham, G. Liu, X. Shen, P. Zong, and J. Yang, "LTE-Advanced: an operator perspective," *Communications Magazine, IEEE*, vol. 50, no. 2, pp. 104–114, 2012.

[7] S. Parkvall, A. Furuskar, and E. Dahlman, "Evolution of LTE toward IMT-Advanced," *Communications Magazine, IEEE*, vol. 49, no. 2, pp. 84–91, 2011.

[8] T. Nakamura, S. Nagata, A. Benjebbour, Y. Kishiyama, T. Hai, S. Xiaodong, Y. Ning, and L. Nan, "Trends in small cell enhancements in LTE Advanced," *Communications Magazine, IEEE*, vol. 51, no. 2, pp. 98–105, 2013.

[9] M. ITU-R, "M. 1645: Framework and overall objectives of the future development of IMT-2000 and systems beyond IMT-2000," tech. rep., 2008.

[10] D. Astely, E. Dahlman, G. Fodor, S. Parkvall, and J. Sachs, "LTE Release 12 and beyond [accepted from open call]," *Communications Magazine, IEEE*, vol. 51, no. 7, pp. –, 2013.

[11] J.-G. Remy, "LTE-SAE: Evolution of GSM towards ≪all IP≫," in *Computational Technologies in Electrical and Electronics Engineering (SIBIRCON), 2010 IEEE Region 8 International Conference on*, pp. 3–3, IEEE, 2010.

[12] E. LTE, "Evolved Universal Terrestrial Radio Access (E-UTRA) and Evolved Universal Terrestrial Radio Access Network (E-UTRAN)](TS 36.300, version 8.11. 0 Release 8), December 2009," *ETSI TS*, vol. 136, no. 300, p. V8.

[13] M. Mohamed, A. Samarah, and M. F. Allah, "Study of performance parameters effects on OFDM systems," *IJCSI International Journal of Computer Science Issues*, vol. 9, no. 3, 2012.

[14] J. Li, X. Wu, and R. Laroia, *OFDMA Mobile Broadband Communications: A Systems Approach*. Cambridge University Press, 2013.

[15] M. Ismail, R. Fauzi, J. Sultan, N. Misran, H. Mohamad, and W. Jabbar, "Performance evaluation of papr in ofdm for umts-lte system," in *Personal Indoor and Mobile Radio Communications (PIMRC), 2012 IEEE 23rd International Symposium on*, pp. 1342–1347, 2012.

[16] M. B. Arun Gangwar, "An overview: Peak to average power ratio in OFDM system & its effect," *International Journal of Communication and Computer Technologies*, vol. 1, no. 2, pp. 22–25, 2012.

[17] G. Berardinelli, L. Ruiz de Temino, S. Frattasi, M. Rahman, and P. Mogensen, "OFDMA vs. SC-FDMA: performance comparison in local area IMT-A scenarios," *Wireless Communications, IEEE*, vol. 15, no. 5, pp. 64–72, 2008.

[18] G. Berardinelli, L. Ruiz de Temino, S. Frattasi, M. Rahman, and P. Mogensen, "OFDMA vs. SC-FDMA: performance comparison in local area imt-a scenarios," *Wireless Communications, IEEE*, vol. 15, no. 5, pp. 64–72, 2008.

[19] C. V. N. Index, "Global mobile data traffic forecast update, 2012–2017 http://www. cisco. com/en," *US/solutions/collateral/ns341/ns525/ns537/ns705/ns827/white_paper_c11-520862. html (Son erişim: 5 Mayıs 2013)*.

[20] H. Ishii, Y. Kishiyama, and H. Takahashi, "A novel architecture for LTE-B: C-plane/U-plane split and phantom cell concept," in *Globecom Workshops (GC Wkshps), 2012 IEEE*, pp. 624–630, IEEE, 2012.

[21] L. Wang, Y. Zhang, and Z. Wei, "Mobility management schemes at radio network layer for lte femtocells," in *Vehicular Technology Conference, 2009. VTC Spring 2009. IEEE 69th*, pp. 1–5, IEEE, 2009.

[22] 3GPP, "Technical specification group services and system aspects; architecture aspects of Home NodeB and Home eNodeB (release 9)," *TR*, vol. 23, p. v9, 2009.

[23] A. Golaup, M. Mustapha, and L. B. Patanapongpibul, "Femtocell access control strategy in UMTS and LTE," *Communications Magazine, IEEE*, vol. 47, no. 9, pp. 117–123, 2009.

[24] M. Yavuz, F. Meshkati, S. Nanda, A. Pokhariyal, N. Johnson, B. Raghothaman, and A. Richardson, "Interference management and performance analysis of UMTS/HSPA+ femtocells," *Communications Magazine, IEEE*, vol. 47, no. 9, pp. 102–109, 2009.

[25] E. Pateromichelakis, M. Shariat, A. Ul Quddus, and R. Tafazolli, "On the analysis of co-tier interference in femtocells," in *Personal Indoor and Mobile Radio Communications (PIMRC), 2011 IEEE 22nd International Symposium on*, pp. 122–126, IEEE, 2011.

[26] N. Saquib, E. Hossain, L. B. Le, and D. I. Kim, "Interference management in OFDMA femtocell networks: Issues and approaches," *Wireless Communications, IEEE*, vol. 19, no. 3, pp. 86–95, 2012.

[27] T. Zahir, K. Arshad, A. Nakata, and K. Moessner, "Interference management in femtocells," 2012.

[28] N. Benvenuto and P. Bisaglia, "Parallel and successive interference cancellation for mc-cdma and their near-far resistance," in *Vehicular Technology Conference, 2003. VTC 2003-Fall. 2003 IEEE 58th*, vol. 2, pp. 1045–1049 Vol.2, 2003.

[29] S. Sen, N. Santhapuri, R. R. Choudhury, and S. Nelakuditi, "Successive interference cancellation: a back-of-the-envelope perspective," in *Proceedings of the 9th ACM SIGCOMM Workshop on Hot Topics in Networks*, p. 17, ACM, 2010.

[30] S.-E. Elayoubi, O. Ben Haddada, and B. Fourestie?, "Performance evaluation of frequency planning schemes in ofdma-based networks," *Wireless Communications, IEEE Transactions on*, vol. 7, no. 5, pp. 1623–1633, 2008.

[31] A. Gusmao, P. Torres, R. Dinis, and N. Esteves, "On SC/FDE block transmission with reduced cyclic prefix assistance," in *Communications, 2006. ICC'06. IEEE International Conference on*, vol. 11, pp. 5058–5063, IEEE, 2006.

[32] R. Dinis, M. Serrazina, and P. Carvallho, "An efficient detection technique for SC-FDE systems with multiple packet collisions," in *Computer Communications and Networks, 2007. ICCCN 2007. Proceedings of 16th International Conference on*, pp. 402–407, IEEE, 2007.

[33] A. Tajer, A. Nosratinia, and N. Al-Dhahir, "Diversity analysis of symbol-by-symbol linear equalizers," *Communications, IEEE Transactions on*, vol. 59, no. 9, pp. 2343–2348, 2011.

[34] N. Benvenuto, R. Dinis, D. Falconer, and S. Tomasin, "Single carrier modulation with nonlinear frequency domain equalization: an idea whose time has come?again," *Proceedings of the IEEE*, vol. 98, no. 1, pp. 69–96, 2010.

[35] N. Benvenuto and S. Tomasin, "Block iterative DFE for single carrier modulation," *Electronics Letters*, vol. 38, no. 19, pp. 1144–1145, 2002.

[36] J.-L. Lu, W. Shu, and M.-Y. Wu, "A survey on multipacket reception for wireless random access networks," *Journal of Computer Networks and Communications*, vol. 2012, 2012.

[37] F. Ganhão, R. Dinis, and L. Bernardo, "Analytical evaluation of iterative packet combining and multipacket detection schemes for SC-FDE," in *Vehicular Technology Conference (VTC Fall), 2011 IEEE*, pp. 1–5, IEEE, 2011.

[38] M. Series, "Guidelines for evaluation of radio interface technologies for IMT-Advanced," tech. rep., ITU, Tech. Rep, 2009.

[39] C. V. Forecast, "Cisco visual networking index: Global mobile data traffic forecast update 2009-2014," *Cisco Public Information, February*, vol. 9, 2010.

[40] M. Etoh, T. Ohya, and Y. Nakayama, "Energy consumption issues on mobile network systems," in *Applications and the Internet, 2008. SAINT 2008. International Symposium on*, pp. 365–368, IEEE, 2008.

[41] X. Wang, A. V. Vasilakos, M. Chen, Y. Liu, and T. T. Kwon, "A survey of green mobile networks: Opportunities and challenges," *Mob. Netw. Appl.*, vol. 17, pp. 4–20, Feb. 2012.

[42] Z. Hasan, H. Boostanimehr, and V. K. Bhargava, "Green cellular networks: A survey, some research issues and challenges," *Communications Surveys & Tutorials, IEEE*, vol. 13, no. 4, pp. 524–540, 2011.

[43] Z. Niu, Y. Wu, J. Gong, and Z. Yang, "Cell zooming for cost-efficient green cellular networks," *Communications Magazine, IEEE*, vol. 48, no. 11, pp. 74–79, 2010.

[44] H. Claussen, L. T. Ho, and F. Pivit, "Leveraging advances in mobile broadband technology to improve environmental sustainability," *Telecommunications Journal of Australia*, vol. 59, no. 1, 2010.

[45] D. Lee, H. Seo, B. Clerckx, E. Hardouin, D. Mazzarese, S. Nagata, and K. Sayana, "Coordinated multipoint transmission and reception in LTE-Advanced: deployment scenarios and operational challenges," *Communications Magazine, IEEE*, vol. 50, no. 2, pp. 148–155, 2012.

[46] F. Pantisano, M. Bennis, W. Saad, and M. Debbah, "Cooperative interference alignment in femtocell networks," in *Global Telecommunications Conference (GLOBECOM 2011), 2011 IEEE*, pp. 1–6, IEEE, 2011.

[47] R. Balasubramaniam, S. Nagaraj, M. Sarkar, C. Paolini, and P. Khaitan, "Cell zooming for power efficient base station operation," in *Wireless Communications and Mobile Computing Conference (IWCMC), 2013 9th International*, pp. 556–560, IEEE, 2013.

[48] R. Balasubramaniam, "Cell zooming techniques for power efficient base station operation," 2012.